筑 波 大 学

博士（医学）学位論文

A novel therapeutic strategy for pancreatic cancer: targeting cell surface glycan using rBC2LC-N lectin-drug conjugate (LDC)

（rBC2LC-N レクチン（レクチン薬剤複合体）を用いた膵癌細胞表面の特異的糖鎖をターゲットにした新規癌治療法の開発）

２０１７

筑波大学大学院博士課程人間総合科学研究科

下村　治

Table of contents

1. Introduction

Cancer-targeting antibody drugs, including antibody-drug conjugates (ADC) (1, 2), are attractive therapies, but their clinical success rates have been limited (3). The targets of these drugs are usually peptides of cell transmembrane proteins; however, it is important to note that cell surfaces are covered by a glycan layer that is referred to as the glycocalyx (4). The glycomes of cancer cell surfaces are often unique, with aberrant glycosylation including sialylation, fucosylation, *O*-glycan truncation, and *N*-and *O*-linked glycan branching (5-7). Therefore, targeting outer-layer glycans might be a more effective cancer-targeting strategy than targeting the underlying core proteins. While carbohydrate-binding monoclonal antibodies have now been investigated for tumour targeting for several decades, none have yet been approved in the clinic (8). Thus, novel powerful therapeutic methods targeting cancer cell surface glycans that are not based on the principal of antigen-antibody affinities should shed light on intractable cancers such as pancreatic ductal adenocarcinoma (PDAC) (9).

Lectins, proteins that recognize glycans and thus have glycan-binding potential, are an alternative to antibodies. However, exogenous lectins, such as those collected from plants, fungi, and snake venom, often have erythrocytic agglutination activity, which has discouraged their application *in vivo* (10). In contrast to the general concept, the extent of

lectin haemagglutination activity is quite variable (10). More than 100 putative endogenous lectins, such as selectin and galectin (12), have been identified in humans (11) and contribute to various physiological processes (10).

In this report, we tested whether lectins could be a drug carrier for cancer therapy that is applicable *in vivo*. We first identified a lectin that possesses specific affinity to the glycans of cancer cell surfaces using a rare and valuable PDAC cell line that has a well-to-moderately differentiated morphology. The selected lectin was then fused to a bacterial toxin to construct a lectin-drug conjugate (LDC), and its prominent cytocidal effect was demonstrated using an *in vitro* assay. The therapeutic effects of LDC on PDAC were tested *in vivo* using a cell line-based xenograft (cell-xeno) model and a patient-derived xenograft (PDX) model.

2. Aim of research

To find out the pancreatic cancer specific glycan and lectins with specific affinity to cancer cells and evaluate the anti-tumour effect of lectin-drug conjugate (LDC) for pancreatic cancer cells both *in vitro* and *in vivo.*

3. Materials and methods

3-1. Cell lines

A total of 6 human pancreatic cancer cell lines with various cell differentiation states in their origin were used. AsPC-1 (CRL-1682, Sep. 19, 2013), BxPC-3 (CRL-1687, Aug. 4, 2015), Capan-1 (HTB-79, July 26, 2013), MIAPaCa-2 (CRL-1420, Sep. 5, 2013), and PANC-1 (CRL-1469, March 4, 2015) were purchased from American Type Culture Collection (ATCC, VA, USA), and SUIT-2 (JCRB1094, July 28, 2015) was obtained from the National Institute of Biomedical Innovation (Osaka, Japan). The morphologies of their clinical PDAC origin were as follows: well-differentiated for Capan-1; and those of the other 5 lines were poorly or poorly moderately differentiated (13). Capan-1, MIAPaCa-2 and AsPC-1 cells were verified by STR-PCR in March 2016 (report number: KBN0366, National Institute of Biomedical Innovation, Osaka, Japan). The remaining cell lines were used within 6 months of purchase and were tested for contamination with mycoplasma.

3-2. Patient samples and tissue collection

Fresh human pancreatic cancer tissue was obtained with patient consent as approved by the Research Ethics Board of the University of Tsukuba. A total of 69 resected pancreatic adenocarcinoma specimens (7 poorly differentiated (P/D) cases, 53 moderately differentiated (M/D) cases and 9 well-differentiated cases) were used in this study. For the use of these clinical samples for research purposes, written informed consent was obtained from all patients, and approval was obtained from the Tsukuba Clinical Research & Development Organization (T-CReDO protocol number: H28-90).

3-3. Lectin microarray

The high-density lectin microarray was prepared as previously described (14). Briefly, proteins from each cell line were prepared from whole-cell lysates of six different wells and fluorescently labelled with the monoreactive dye Cy3 (GE Healthcare). Then, 0.5 μg/ml Cy3-labelled lysate was added to each well of a microarray plate, and the plate was incubated at 20°C overnight. Fluorescence images were then acquired using an evanescent field-activated fluorescence scanner (GlycoStation^{TM} Reader; GlycoTechnica LTD, Yokohama, Japan). The fluorescence signal of each spot was quantified using

Array-Pro Analyser version 4.5 (Media Cybernetics, Bethesda, MD, USA), mean-normalized, log-transformed, and analysed via the average linkage method using Cluster 3.0 (yellow: high; black: intermediate; blue: low).

3-4. Lectin staining

Lectin histochemistry: Antigen retrieval in 2-μm slide sections of formalin-fixed and paraffin-embedded (FFPE) tissues was performed by autoclaving, endogenous peroxidase activity was blocked with 3% H_2O_2 with methanol, and horseradish peroxidase-labelled rBC2 was applied and visualized by applying the chromogen diaminobenzidine (Nichirei, Japan). The clinical cases were judged as 0, 1+, 2+, 3+ with regard to rBC2 reactivity, and the correlation with cell differentiation was assessed.

Live-cell staining by rBC2 lectin: Live cells were incubated for 12 h in medium containing FITC-conjugated rBC2 LNC (1 μg/ml); images were captured using a BIOREVO BZX-710 fluorescence microscope (KEYENCE).

3-5. Production of rBC2-PE38

The recombinant N-terminal domain of BC2L-C (rBC2LC-N) (156 amino acids) was fused to a truncated form of the catalytic domain of pseudomonas exotoxin (PE) A

(399–613 residues; 215 amino acids) carrying a C-terminal 6x-His tag (HHHHHH) and a KDEL sequence via a ten-amino-acid linker (GSG3)2 (Fig. 2A). The generated rBC2-PE38 (371 amino acids) was expressed in *E. coli* and purified via one-step affinity chromatography on an L-fucose-Sepharose column. The yield was 10 mg/l of bacterial culture. rBC2-PE38 was detected as a major band at the predicted molecular weight of 54 kDa by SDS-PAGE in the presence and absence of 2-mercaptoethanol (Supplementary Fig. S1).

3-6. Cell assays

Lectin binding analysis: Cells were harvested and stained with various concentrations of rBC2-FITC for 30 min on ice. The MFI of the cells was determined using an LSR Fortessa X-20 flow cytometer. The data were analysed using a nonlinear regression fitting programme in GraphPad Prism 6 (GraphPad Software Inc., La Jolla, CA, USA).

MTT assay: The cytotoxicity of rBC2-PE38 was measured in a cell viability assay using WST-8 (Dojindo Molecular Technologies) as recommended by the manufacturer. Cells were seeded on 96-well plates at 5×10^3 cells/well. After incubation

for 24 h, rBC2 or rBC2-PE38 was applied to the medium at the indicated concentrations (0.1 pg/ml to 10 μg/ml). After further incubation for 48 h, the culture medium was replaced with the appropriate fresh medium, and the cells were incubated for an additional 24 h. We used 48 h + 24 h and not a continuous 72 h because many cells died after 48 h due to the action of LDC, which was internalised into cells during the first 48 h. Cell viability was then assessed via an MTT assay (WST-8) according to the manufacturer's instructions. After solubilisation of the purple formazan crystals, absorbance was measured at 450 nm (background wavelength, 650 nm) using a plate spectrophotometer. The IC_{50} was calculated using GraphPad Prism 6.

3-7. Haemagglutination assay

Blood samples were obtained from 4 healthy volunteers of each blood type, i.e., A, B, O, and AB. A 5-ml aliquot of freshly whole blood was washed 3 times with 20–25 ml of PBS (centrifugation at 500 g for 5 min, followed by removal of the plasma and white cell ghost layer at the top of the pellet). The suspension of untreated (without using trypsin) erythrocytes was then mixed with an equal volume of incubation buffer (0.1 M acetate buffer containing 1 mM $CaCl_2$, pH 5.5) containing 1 unit/ml neuraminidase (from *C. welchii* Sigma N2876) and incubated at 37°C for 1 h with occasional shaking. All

samples were again washed 3 times with PBS and then prepared as a 2% (v/v) erythrocyte suspension in PBS. Concanavalin A or rBC2 lectin solution (50 μg/ml) was applied to the left well of a U-shaped 96-well plate, and a series of two-fold dilutions were prepared in a horizontal line. The same volume of erythrocyte suspension was applied to each well, and agglutination was observed.

3-8. Toxicology study of rBC2-PE38 (LDC) in wild-type mice

To evaluate the LD_{50} (50% lethal dose) of LDC, female wild-type mice (5–6 weeks old, 18-20 g, Charles River Laboratories International, Japan) were given an intraperitoneal (i.p.) or intravenous (i.v.) injection with a single dose of 1.0 to 15.0 μg of rBC2/mouse or rBC2-PE38/mouse (50 to 750 μg/kg) in 300 μl of PBS. The mice were observed for survival until day 14.

3-9. Animal models of PDAC

Animal experiments were conducted in compliance with the ethical regulations approved by the Animal Care Committee, University Health Network, University of Tsukuba, Tsukuba, Ibaraki, Japan.

Subcutaneous cell xenograft model: A total of 3×10^6 Capan-1 or SUIT-2 cells were subcutaneously injected into female nude mice (BALB/c nu/nu, 6 to 8 weeks old, CLEA Japan, Tokyo, Japan).

Subcutaneous patient-derived xenograft (PDX) model: Fresh human pancreatic cancer tissue originated from a nodules of liver metastasis of clinical PDAC that showed moderately-to-poorly differentiated morphology was implanted into subcutaneous pockets on the back skin of CB17/Icr-scid/SCID mice (female, 6 to 8 weeks old, CLEA Japan, Tokyo, Japan). After the establishment of 1st-generation subcutaneous nodules, the tumour nodules were minced into 2-mm cubic fragments, and 3 pieces were implanted into subcutaneous pockets on the back skin of SCID mice. This PDX nodules show moderately differentiation in morphology.

Pancreatic orthotopic model: Nude mice were anesthetized with isoflurane, a laparotomy was created using a left lateral abdominal incision, and the pancreas was exteriorized. Four tumour pieces (approximately 2 mm in diameter) obtained from peritoneal disseminated Capan-1 nodules were transplanted to the body of the pancreas and secured with absorbable surgical sutures.

Peritoneal dissemination model: Nude mice were inoculated with Capan-1 or SUIT-2 cells by i.p. injection of 2.0×10^6 cells suspended in 100 µl of PBS. On day 14, 2 mice were sacrificed to confirm the establishment of disseminated cancer nodules. The remaining mice were then randomly allocated to 4 groups.

3-10. rBC2-PE38 (LDC) treatment for *in vivo* PDAC mouse models

Direct injection (d.i.) to subcutaneous cell xenograft models and a PDX model. A direct injection (d.i.) of 40 ng, 1 µg or 5 µg of LDC in 100 µl of PBS was performed a total of 4 times near the subcutaneous tumours on days 14, 18, 22, and 26. For the control, 100 µl of normal saline was injected. The tumour volume was determined every day for 2 weeks using the following formula: $(\text{width})^2\times(\text{length})/2$. On day 34, the subcutaneous tumours were excised for weight measurements.

i.p. and i.v. injection of LDC to subcutaneous PDX models. A total of 1 µg LDC was administered in 100 µl of PBS via i.p. injection (n=4 each) or i.v. injection via the tail vein for a total of 8 times on days 14, 17, 19, 22, 24, 26, 29 and 31. On day 36, the subcutaneous nodules were excised for weight measurements.

i.p. and i.v. injection of LDC to orthotopic models. The mice were treated and evaluated on a treatment schedule identical to that of the cell xenograft models, using 1 μg or 5 μg of LDC (n=5 each). On days 21, 24, 28 and 31, 1 μg of LDC was administered i.p. or i.v. via the tail vein. On day 45, the mice were sacrificed for the observation of abdominal status and tumour weight measurement.

i.p. and i.v. injection to peritoneal dissemination models. The Capan-1 peritoneal dissemination mouse models were treated by injection of 1 μg of rBC2 lectin without PE38, 40 ng of LDC or 1 μg of LDC in 100 μl of PBS by i.p. or i.v. injection via the tail vein a total of 4 times on days 14, 18, 22, and 26 (n=4 each). On day 30, the mice were sacrificed for manual counting of the disseminated nodules. The Kaplan-Meier survival curves were calculated using 36 nude mice. At 14 days after the Capan-1 cell injection, 4 groups of mice (n=9 each) were treated on days 1, 5, 9, and 13 with control, 40 ng of LDC via i.p. injection, 1 μg of LDC via i.p. injection, or 1 μg of LDC via i.v. injection.

3-11. Statistical analyses

A heat map of the clustering analysis results was constructed using Java TreeView. Differences in the lectin signal between the two arbitrary data sets were evaluated using Student's t-test in SPSS Statistics 21.0 (SPSS Inc.). Significantly different lectin signals or glycosyltransferase expression levels were selected if they satisfied a familywise error rate (FWER) of < 0.001 according to the Bonferroni method. Applied statistics included the unpaired Student's *t*-test and the Mann-Whitney *U* test. $P<0.05$ was considered to indicate significance. Kaplan-Meier curves (statistically analysed by the log-rank test) and LDC IC50 values of were calculated using GraphPad Prism 6; other analyses were performed using SPSS 21.0 (SPSS Inc.).

4. Result

4-1. Selection of PDAC cell lines that display clinical PDAC and cancer stem-cell-like characteristics

For cancer cell glycome analysis, clinical PDAC samples are limited in terms of sample availability and quality due to the typical histological characteristics of PDAC, which include the presence of epithelial cancer cells forming ductal glands (g++) surrounded by abundant stromal components (s++) (Fig. 1A). We therefore began the experiments by selecting a cell line that represents the dominant morphological properties of clinical PDAC when grown *in vivo*. Only Capan-1 cells strongly exhibited organized gland formation (g++) and dense stromal proliferation (s++) (Fig. 1B). The expression of the known pancreatic cancer stem cell markers CD24, CD44, EpCAM, and CD133 (15, 16), as revealed by flow cytometry analysis, indicated that the Capan-1 line was positive for 3 markers and was the only cell line to show CD 133 positivity (Supplementary Fig. S2). Therefore, we considered Capan-1 to be a rare PDAC line that maintains well-to-moderately differentiated tumour features and thus represents the dominant morphology of clinical PDAC characteristics. In fact, although most clinical human PDACs are well or well-to-moderately differentiated cancers according to histology, and poorly or moderate-to-poorly differentiated cancers represent only 10-15% of cases, most available

PDAC cell lines are derived from poorly or moderate-to-poorly differentiated cancers (13).

4-2. High-density lectin microarray analysis of 6 types of PDAC cell lines

Glycan expression in Capan-1 cells, in which we have focused as the tester cell line that may represent PDAC glycan expressions, was compared with that in 5 other cell lines using high-density lectin microarrays (14). A representative heat map demonstrated that Capan-1 and BxPC-3 cells cluster on the same branch of a tree diagram, separate from the branch that includes the other 4 cell lines (Fig. 1C). Of the 96 lectins tested, the top 10 lectins with significantly different signal intensity in the Capan-1 cell line were identified; these included 8 lectins with increased reactivity and 2 lectins with decreased reactivity (Supplementary Fig. S3 and Supplementary Table S1). The most prominent difference was found in the case of the rBC2LC-N (recombinant N-terminal domain of BC2L-C) lectin (Fig. 1D), a TNF-like lectin that was originally identified in the gram-negative bacterium *Burkholderia cenocepacia* and that specifically binds to fucosylated glycan epitopes of H type 1/3/4 trisaccharides (17).

4-3. The rBC2 LC-N lectin exhibited specific affinity for Capan-1 cells and clinical

PDAC samples

The affinity between the rBC2LC-N lectin and Capan-1 cell glycan was further confirmed by live-cell staining (Fig. 1E), flow cytometry analysis using FITC-labelled rBC2LC-N (Fig. 1F and Supplementary Fig. S4), and histochemical staining of an *in vivo* mouse cell line-derived xenograft model with labelled rBC2LC-N (Fig. 1G and Supplementary Fig. S5). Each experiment revealed similar strong reactivity of the rBC2LC-N lectin to Capan-1 cells (Fig. 1E-G). To address whether reactivity with the rBC2LC-N lectin is specifically associated with Capan-1 cells or whether it can be expanded to general clinical PDAC, we analysed 69 human clinical PDAC specimens by rBC2LC-N lectin histochemical staining. The representative staining patterns of 3 clinical PDAC of poorly (P/D), moderately (M/D) and well-differentiated (W/D) specimens are shown in Fig. 1H. In 7 P/D cases, 6 were weakly positive (1+) for rBC2 staining, whereas in 9 W/D cases, 7 were strongly (2+) or very strongly (3+) positive. M/D cases comprised the majority (53 cases) of the 69 clinical PDAC cases, and their rBC2 staining was as follows: 1+ in 18 cases, 2+ in 25 cases and 3+ in 10 cases. The surrounding stromal components were negative for rBC2 staining (Fig. 1H).

For the top 10 lectins with the highest differences in specific affinity, lectin histochemical analysis of serial sections of clinical PDAC specimens demonstrated that

rBC2LC-N showed the most prominent contrast in terms of its intensive affinity for cancer cells and its lack of affinity for stromal fibroblast cells (Supplementary Fig. S6). Our data indicate that a fucosylated glycan epitope (H type 1/3/4) that is recognized by the rBC2LC-N lectin may serve as a promising therapeutic target for PDAC.

4-4. Construction of LDC and its cytocidal activity *in vitro*

With the aim of utilizing the rBC2LC-N lectin (rBC2) as a therapeutic drug carrier, a 38-kDa region of the catalytic domain of *Pseudomonas aeruginosa* exotoxin A (PE A) was fused with the lectin sequence to construct LDC (rBC2-PE38) (18) (Fig. 2A). The dissociation constant (Kd) values for rBC2 indicated high-affinity binding of the conjugate only to Capan-1 cells (Kd: 171.4 nmol/l, Fig. 2B). The cytocidal effect of LDC was measured using an MTT assay; the 50% inhibitory concentration (IC_{50}) of LDC against Capan-1 cells was 1.04 pg/ml (0.0195 pmol/l, Fig. 2C), nearly 1000 times lower than that of conventional immunotoxins, which generally have IC_{50} values on the order of ng/ml (Supplementary Table S2). The other 5 cell lines that displayed no affinity for the rBC2LC-N lectin showed moderate to negative cytocidal effects (Fig. 2D). Because internalization into the cell cytoplasm is a key indispensable step for the cytocidal toxicity of PE toxin (19), the endocytosis of rBC2 lectins was observed. One hour after application

of the conjugate, the cell surfaces of the Capan-1 cells were surrounded by rBC2 lectins (Fig. 2E). Endocytic vesicles containing rBC2 lectin were visible inside Capan-1 cells at 24 h and more conspicuous at 48 h. In contrast to Capan-1 cells that possess positive affinity for rBC2 lectins, the negative control cell line (SUIT-2), which has no affinity for rBC2 lectins, showed no fluorescence intensity on the cell membrane at 24 h and no endocytic vesicles inside the cytoplasm at 48 h.

4-5. Safety of intravital administration of LDC (rBC2-PE38)

We questioned whether our selected lectin would be a safe and effective drug carrier that could be administered to cancer patients because lectins are often defined by their cell agglutination activities. We evaluated the reactivity of the rBC2LC-N lectin on the surface of non-cancerous abdominal organs in mice (Fig. 3A) and confirmed that rBC2LC-N exhibited negative reactivity for the entire parietal peritoneum and the serosal membranes of visceral organs. The disseminated cancer nodules of Capan-1 cells were confirmed to be strongly positive for rBC2LC-N reactivity. Importantly, an *in vitro* haemagglutination test of erythrocytes from mice and a human volunteer (blood type A) demonstrated that the rBC2LC-N lectin did not induce haemagglutination even at a high concentration of 50 μg/ml, in contrast to the obvious aggregation caused by the

concanavalin A (Con A) lectin at 1.56 μg/ml in mouse and human erythrocytes (Fig. 3B). LDC (rBC2-PE38) slightly affected haemagglutination at very high concentrations, as demonstrated by a positive result at 25 μg/ml in mouse erythrocytes and 12.5 μg/ml in human erythrocytes (Fig. 3B). Identical results were obtained for human erythrocytes of other blood types, including type B, AB and O (Supplementary Fig. S7). In addition, the rBC2LC-N lectin staining of human red blood cells contaminating clinical PDAC slides revealed that all red blood cells were negative, indicating that human red blood cells are likely to be negative for the H type 1/3/4 motif (Fig. 3C and Supplementary Fig. S8). Notably, white blood cells (* with blue nuclei) were also negative for rBC2LC-N reactivity. When the LDC 50% lethal dose (LD50) was analysed by i.p. and i.v. administration, acceptable values were estimated to be 7.14 μg/mouse (424.8 μg/kg) for i.p. and 7.22 μg/mouse (429.6 μg/kg) for i.v. (Fig. 3D). Administration of the BC2LC-N lectin without conjugated toxin did not cause death at any dose tested up to 15 μg/mouse (892.5 μg/kg), either i.p. or i.v. Based on these observations, we were confident that at least the i.p. injection, and likely also the i.v. injection, of LDC would be safe for mouse models *in vivo*.

4-6. Therapeutic effect of LDC in various mouse tumour models

1. Subcutaneous xenografts treated by local injection

In cell line-based models, Capan-1 xenografts (positive for the H type 1/3/4 glycan epitope) were significantly diminished by LDC direct injection (d.i.) (Fig. 4A1-3). However, regarding SUIT-2 xenografts, which exhibit no affinity to the rBC2LC-N lectin, LDC injection did not reduce the tumour sizes except when the dose reached 5 μg/mouse (Fig. 4B1-3). In a more clinically relevant patient-derived xenograft (PDX) model, tumours decreased in size after LDC administration in a dose-dependent manner (Fig. 4C1-3).

2. Subcutaneous PDX xenografts treated by i.p. or i.v. injection

The anti-tumour effects of LDC administration via the i.p. or i.v. routes for subcutaneous tumours of the PDX model are shown in Fig. 4D1-3. Although these tumours grow rapidly in the control group (normal saline i.p.), LDC treatment groups that received a total of 8 treatments showed reduced growth with either i.v. or i.p. administration. The average tumour weights at day 36 were 991 mg in the control group, whereas those of i.p. and i.v. administration group were 540.6 and 686.6 mg, respectively ($P<0.01$ and $P<0.05$, respectively, relative to control).

3. Pancreatic orthotopic xenografts treated by i.p. or i.v. injection

The effects of 4 LDC treatments (1 μg/mouse) administered via i.p. or i.v. for orthotopic tumours are shown in Fig. 4E1-4. The average tumour weights after i.p. and i.v. administration were 130.8 mg and 203 mg, respectively ($P<0.001$ and $P<0.05$, respectively, relative to the control value of 390 mg). Macroscopic metastases to the liver, spleen or abdomen occurred frequently in the control groups (3-4/5 mice) but were rare in the LDC treatment groups (0-2/5 mice).

4. Peritoneal dissemination models treated by i.p. or i.v. injection

By day 14, peritoneal disseminated nodules had grown to a visible size and measured 1–3 mm (Fig. 5A). In the Capan-1 group, significantly fewer disseminated nodules were observed upon treatment with either 40 ng of LDC/mouse or 1 μg of LDC/mouse (Fig. 5B). In the SUIT-2 group, for which rBC2 exhibited no affinity, LDC had no effect (Fig. 5C). In the control groups, the peritoneal cavities of the mice contained abundant cancer cells, whereas there were no cancer cells in the peritoneal cavities of the mice in the 1 μg of LDC/mouse treatment group (Fig. 5D). At day 45, the weights of the mice were significantly improved both in i.v. and i.p. administration (Fig. 5E). The effect of LDC administration occurred even after i.v. administration, as shown by the absence

of disseminated nodules (Fig. 5F-1), ascites, and liver metastasis (Fig. 5F-2). Finally, we addressed whether glycan-targeting LDC therapy could cure PDAC in the mouse model of PDAC (Fig. 5G). The median survival of the control group was 62 days, with a 90-day survival rate of 0% (0/9). In contrast, administration of four i.p. injections of 1 μg of LDC resulted in a 90-day survival rate of 78% (7/9) and improved the median survival time significantly (105 days) ($P<0.0001$). The effects of four i.v. injections of 1 μg of LDC were comparable to those of i.p. injection, resulting in a 56% (5/9) 90-day survival rate and a median survival time of 90 days.

5. Discussion

Thus far, the potential of lectins for *in vivo* cancer treatment have not been well tested, likely due to the common belief that all lectins mediate harmful haemagglutination. In this study, we found a specific affinity between the rBC2LC-N lectin and PDAC cell surface glycans (fucosylated glycan epitopes of H type 1/3/4 trisaccharide), and this lectin was shown to be a safe and efficient drug carrier in cancer treatment.

The identification of rBC2LC-N as the most highly reactive lectin in PDAC was an unexpected coincidence because we previously reported that rBC2LC-N specifically interacts with induced pluripotent stem (iPS) and embryonic stem (ES) cells but not with

differentiated somatic cells (20). The serendipitous finding that an rBC2LC-N fucose-binding lectin displays affinity for PDAC and iPS/ES cells indicates that consensus glycan modification of membrane proteins or lipids containing H type 1/3/4 glycan on PDAC cells plays a crucial role in the formation and development of cancerous tissue. The specific affinity between LDC and cancer cell surface H type 1/3/4 glycan was confirmed by competitive inhibition by adding free rBC2LC-N lectin and free glycan (=fucose) (Supplementary Fig. S9).

One critical question has been whether the rBC2LC-N lectin can safely be administered to cancer patients because lectins are initially defined by their blood agglutination activities (10). This concern was addressed using an *in vitro* haemagglutination assay; the results showed that the rBC2LC-N lectin did not induce the aggregation of human erythrocytes (Fig. 3B and Supplementary Fig. S7), and the negative rBC2LC-N staining of human red blood cells contaminating 69 clinical PDAC specimens is shown (Fig. 3C and Supplementary Fig. S8). This finding might be explained by the fact that the ABO blood type glycans on red blood cells contain predominantly H type 2 trisaccharide motifs in which Gal and GlcNAc are connected via beta-1-4 glycosidic bonds (21). rBC2LC-N is known to bind only H type 1/3/4 trisaccharide motifs and not H type 2 motifs (17). The biosynthesis of H type 1 trisaccharide motif is completed via

fucose addition to galactose in type 1 (Gal-GalNAc), or H type 3/4 are generated by fucosylation of type 3/4 disaccharide (Gal-GalNAc) by fucosyltransferases (Fig. 6A) (17). Moreover, the rBC2LC-N lectin was administered to mice without notable adverse events, further indicating that this lectin alone does not induce blood coagulation *in vivo* (Fig. 3D). Based on our experimental data and the literature, we are confident that the rBC2LC-N lectin could be administered via the intravenous route without inducing haemagglutination.

The next issue should be the potential non-specific attachment of rBC2LC-N to non-cancerous normal tissues other than red blood cells. Fucose modification of glycans is one of the representative cancer-specific changes in glycosylation (5); however, fucosylated type 1/3/4 glycan epitopes are also found in non-cancerous epithelial cells of the gastrointestinal, respiratory, and reproductive tracts (22). Our results obtained using rBC2LC-N lectin staining also revealed positive staining of epithelial cells in the exocrine glands of the stomach, duodenum, small intestine, colon and genitourinary tract, presumably associated with secreted mucin (Fig. 3A). However, we considered the risk of LDC affinity for these cells to be negligible after administration via the i.p. route because mucin secretion predominantly occurs on the internal luminal surface of halo organs, and the outer serosal surfaces of these organs are negative for rBC2LC-N

reactivity. As expected, i.p. administration of LDC resulted in a prominent tumour elimination effect in a mouse model of peritoneal dissemination of PDAC without adverse events. Though the rBC2 reactivity to human organs showed similar distribution with those of mouse (Supplementary Fig. S10), the different statuses of glycosylation and fucosylation between species, i.e., human and mouse, may result in the potential toxicity of LDC in the human setting. Even after i.v. administration, distribution to non-cancerous organs should be very limited with the enhanced permeability and retention (EPR) effect, which results in predominant delivery of large molecules to cancer tissues via the damaged endothelial cell linings of capillaries in the region of the tumour (23). In fact, the i.v. injection of 1 μg of LDC/mouse also shrank tumours in the orthotopic (Fig. 4E) and peritoneal dissemination model of Capan-1 cells (Fig. 5F) and subcutaneous PDX tumour (Fig. 4D) with an efficacy identical to that of i.p. injection without notable adverse events. However, it should also be noted that the EPR effect showing the predominant accumulation of LDC in PDX tumours in mouse models may not be reproduced in clinical PDAC, because human PDACs are known to be hypoperfused and poorly vascularized compared with xenotransplanted tumours (24, 25).

Compared with the affinity of antibodies for peptide antigens (Kd=0.1-10 nmol/l), the affinity of lectins for their target glycans is typically weaker (Kd=100-1000

nmol/l). However, LDC possesses the following notable advantages (shown schematically in Fig. 6B): i) the target glycans are located at the outermost coatings of cancer cells, known as glycocalyx, conferring easy access for targeting drugs; ii) the cancer cells possess abundant glycan sites for interaction with LDC, including branched glycan chains attached to multiple different core proteins; iii) the small size of the lectin should be beneficial for drug endocytosis; and iv) the glycolipids are also the binding target of LDC, and the very close proximity of glycolipids to the cell membrane should be favourable for drug endocytosis. As a comprehensive result, the lectin drug displayed a remarkable IC_{50} value of 0.0195 pmol/l l, nearly 1000 times lower than the IC_{50}s of conventional immunotoxins, which are on the order of ng/ml (Supplementary Table S2); thus, the lectin drug provides a prominent cancer therapeutic effect. As lectins can be generated in an economical bacterial system, lectin-based drugs should be advantageous from the viewpoint of medical economics in comparison to antibody-based drugs that require costly eukaryotic cells for their production (26).

rBC2LC-N may be a unique lectin that lacks typical haemagglutination activity. However, the rapid improvement in lectin engineering technologies (27) will provide control over the harmful adverse effects of some lectins, and synthetic lectin technologies will permit the development of *de novo* lectins with ideal characteristics as drug carriers.

This study provides new insight into cancer treatments that might serve as alternatives to expensive antibody-based drugs. Moreover, the application of tumour-targeting lectins might be expanded by coupling them to small-molecule agents or to nanoparticles, potentially leading to breakthroughs in cancer treatment.

6. Conclusion

Targeting cancer specific glycans using lectin promised great advancement in effective drug delivery and our lectin-drug conjugate (LDC) using rBC2LC-N lectin showed a convincing anti-tumour effect for pancreatic cancer cells both *in vitro* and *in vivo*.

7. Figures

Figure 1

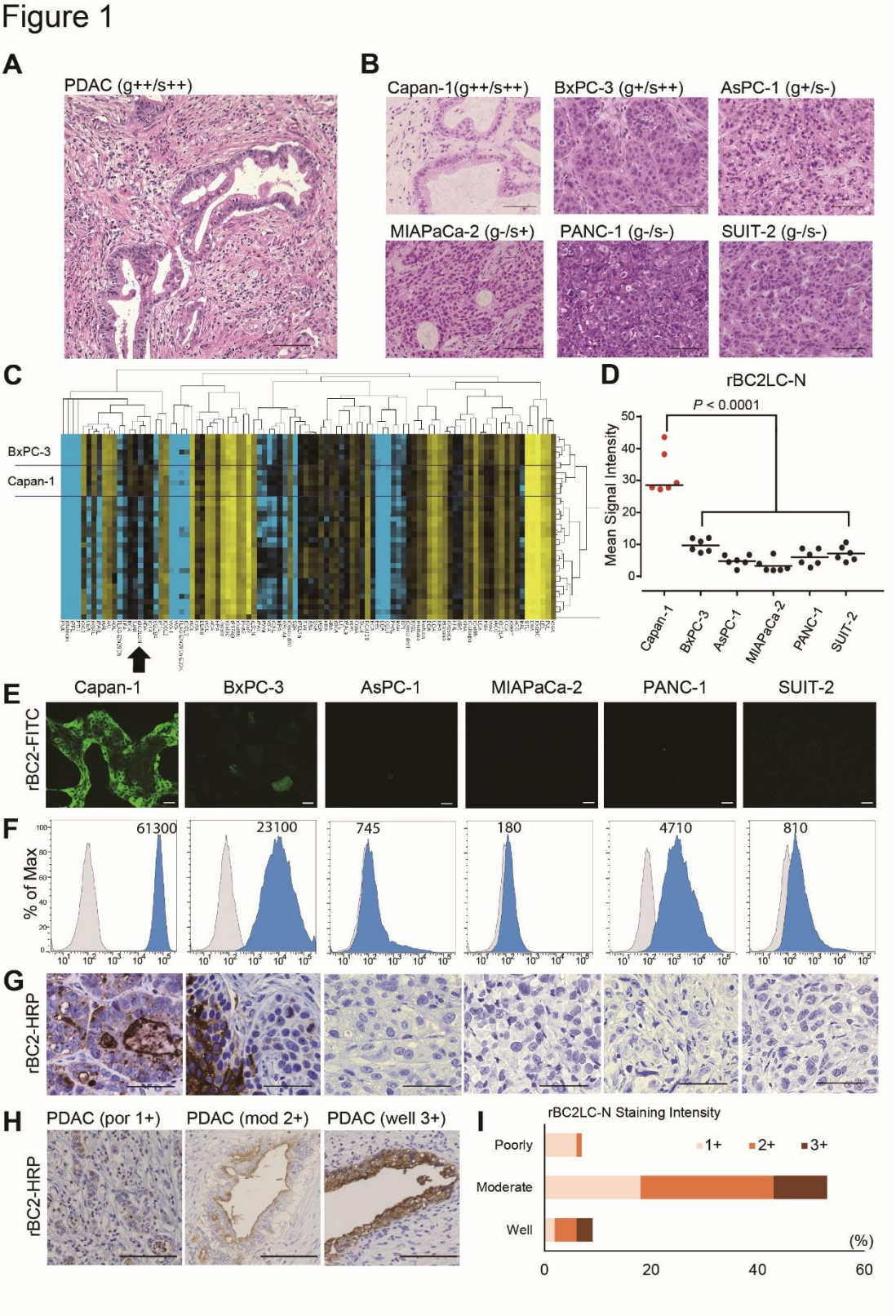

Fig. 1. **Screening for lectins that specifically bind to PDAC.**

A, The pathology of a typical PDAC specimen consists of a cluster of ductal spreading cancer cells with abundant stromal components, defined as gland formation (g++) and stromal induction (s++). **B,** The morphologies of the 6 pancreatic cancer cell lines in mouse xenografts with respect to gland formation (g++, + or -) and stromal induction (s++, + or -). Capan-1 cells exhibited strong, organized gland formation (g++) and dense stromal proliferation (s++). **C,** High-density lectin microarray analysis of 96 various lectins was performed on 6 PDAC cell lines (n=6 protein samples for each cell line, technical replicates). A heat map of the clustering analysis (yellow: high; black: intermediate; blue: low) placed BxPC-3 and Capan-1 cells on an identical branch of the tree diagram (above the line). The position of the rBC2LC-N lectin is indicated by an arrow. **D,** For each of the 96 lectins assessed, the signal intensity in the Capan-1 cell line was compared with that of the other 5 cell lines. The rBC2LC-N lectin exhibited the most robust difference (two-tailed unpaired Student's *t*-test). The top 10 lectins that showed specific affinity differences in Capan-1 cells are described in Supplementary Figure S3 and Table S1. **E,** The specific affinity of rBC2LC-N for Capan-1 cells in the lectin microarray was further confirmed by live-cell staining using FITC-labelled rBC2LC-N (scale bar, 50 μm). **F**, rBC2LC-N reactivity analysis by flow cytometry confirmed that

Capan-1 cells displayed the highest affinity for rBC2LC-N, as indicated by an MFI of 61300. **G**, Lectin histochemistry of cell-based xenograft models demonstrated strong staining for rBC2LC-N in Capan-1 xenografts (brown signal and blue counterstaining with haematoxylin) and mosaic staining in BxPC-3 xenografts. The remaining 4 xenografts were negative for rBC2LC-N (scale bar, 100 μm). **H,** rBC2LC-N lectin histochemistry in human clinical PDAC specimens. Representative micrographs of 3 cases, including P/D with weak (1+) staining, M/D with moderate (2+) staining, and W/D with strong (3+) staining. **I**, Among the 69 human clinical PDAC cases, P/D cases tended to show weak staining with rBC2, and W/D cases showed moderate to strong staining. The primary differentiation was M/D (53/69), which demonstrated similar distribution as W/D cases.

Figure 2

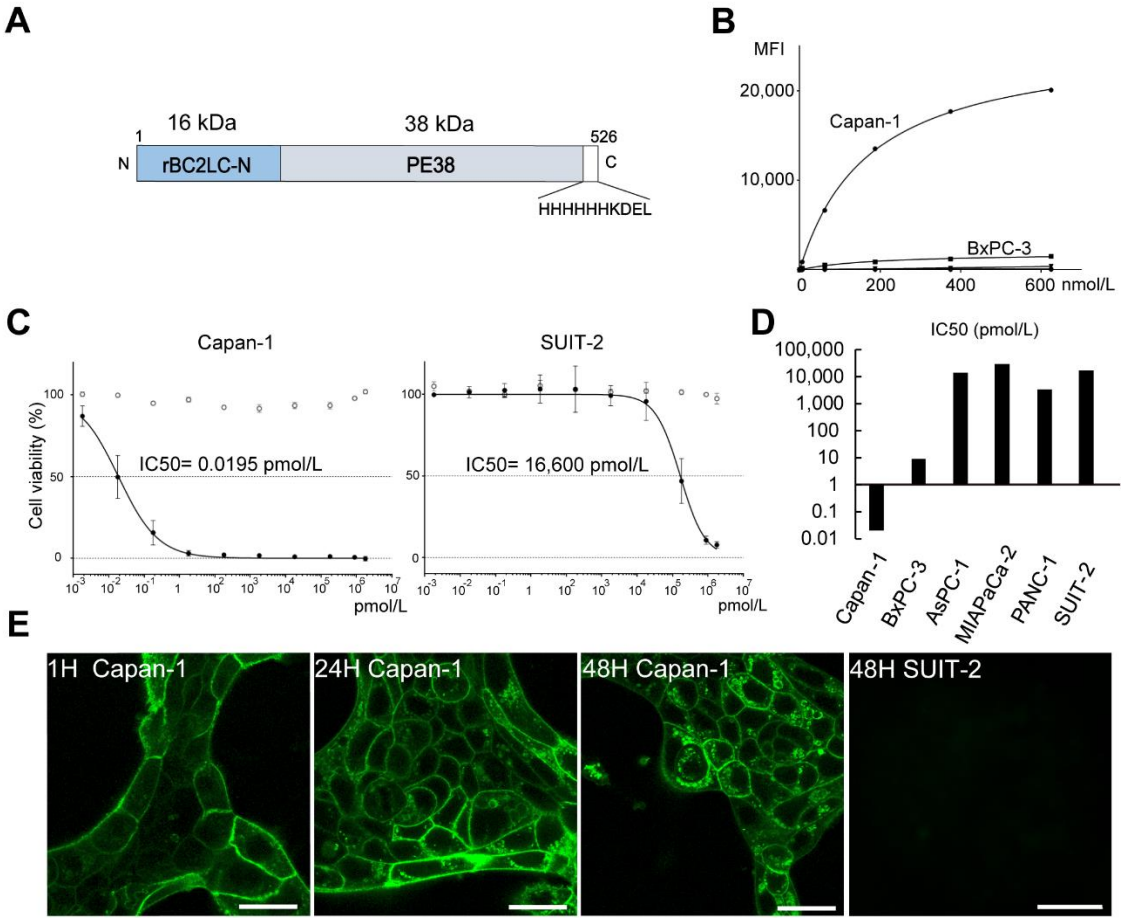

Fig. 2. LDC (rBC2-PE38) and its *in vitro* cytotoxicity against PDAC cells.

A, The 54-kDa LDC (rBC2-PE38) molecule contains a 16-kDa rBC2LC-N (recombinant N-terminal domain of BC2 L-C lectin) region and a 38-kDa region representing the catalytic domain of *Pseudomonas* exotoxin A (PE38). **B,** Binding affinity of the rBC2LC-N lectin in 6 PDAC cell lines. Only Capan-1 cells (Kd=171.4 nmol/l) demonstrated high affinity for rBC2LC-N, whereas Kd values could not be estimated for the other cell lines. **C,** MTT assays using WST-8 were performed to more precisely evaluate the *in vitro* cytotoxic effect of LDC (black circle). The IC_{50} value against Capan-1 cells (0.0195

pmol/l=1.04 pg/ml) was substantially lower than that against SUIT-2 (16,600 pmol/l). **D,** Summary of LDC IC_{50} values against 6 PDAC cell lines. Capan-1 showed marked sensitivity, BxPC3 showed intermediate sensitivity (IC50=9.24 pmol/L=520 pg/ml), whereas the remaining 4 cell lines had IC50s on the order of 10,000 pmol/l, indicating no significant affinity for rBC2LC-N. **E,** Live Capan-1 cells after incubation with fluorescently labelled rBC2. At 1 h, confocal laser microscopy showed that the cell surface membranes were covered with rBC2-FITC, but rBC2-FITC had not been ingested by the cells. After 24 h, fluorescent deposits were observed inside the cells, and these became more conspicuous at 48 h (scale bar, 25 μm). A negative control cell line (SUIT-2) that has no affinity for rBC2 lectins showed no fluorescence intensity on the cell membrane at 24 h and no endocytic vesicles inside the cytoplasm at 48 h.

Figure 3

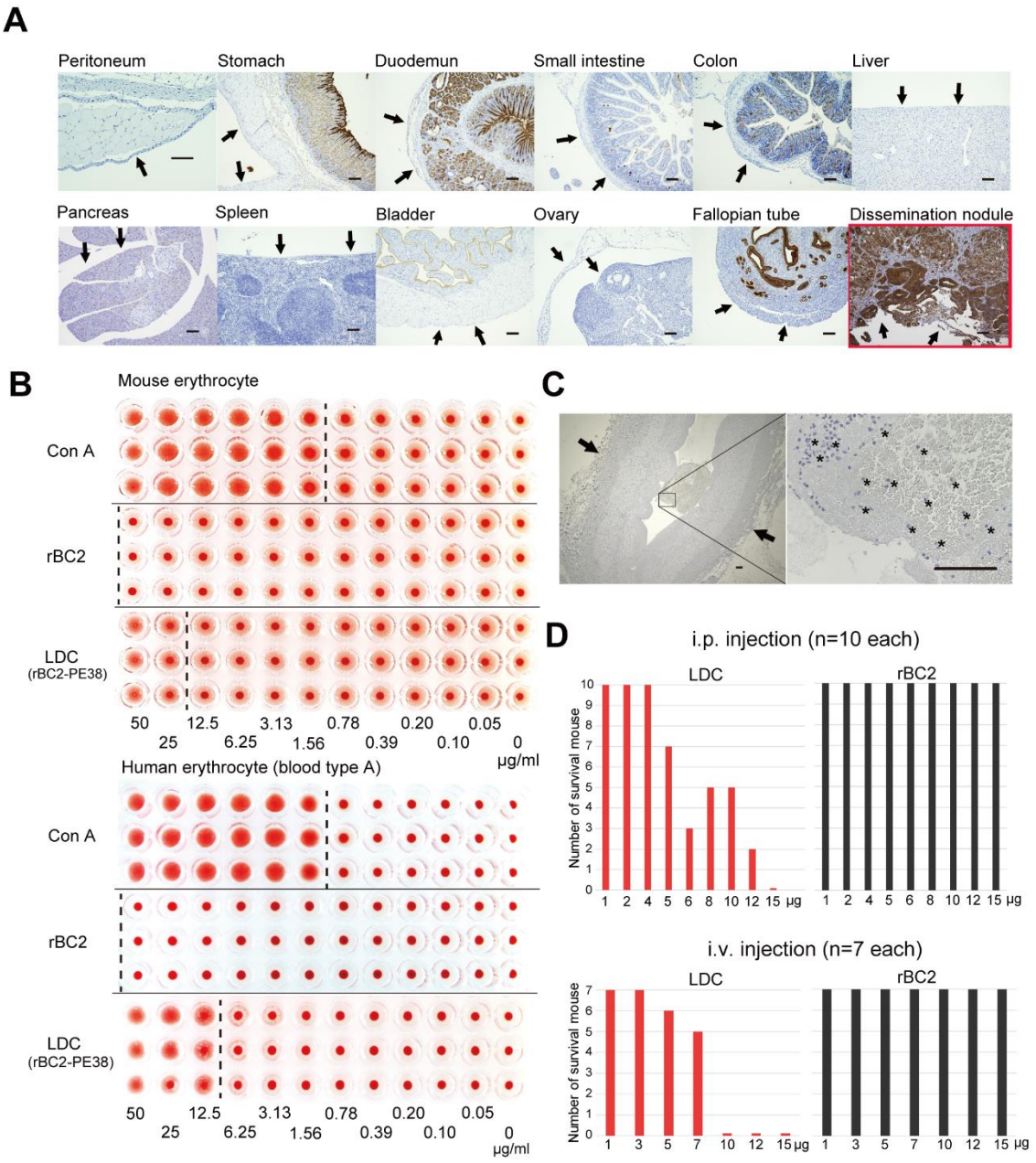

Fig. 3. Safety of LDC administration.

A, rBC2LC-N lectin reactivity to mouse organ surfaces that might be exposed to LDC administered via the i.p. route. Negative reactivity to the entire parietal peritoneum and the visceral peritoneum of hollow, solid and genitourinary organs (arrows) were

confirmed, in contrast to the strong positivity in the Capan-1 disseminated cancer nodules. Positive reactivity to rBC2LC-N in epithelial cells on the internal surface of the hollow organs (strongly in the stomach, duodenum and fallopian tube and weakly in the small intestine and colon) can be ignored in i.p. administration because these cells do not encounter LDC when injected via the i.p. route. (scale bar, 100 μm) **B,** Haemagglutination assay of rBC2LC-N and LDC. The rBC2LC-N lectin alone did not induce erythrocyte aggregation from mice and a human volunteer, even at an extremely high concentration of 50 μg/ml. A positive control with concanavalin A (Con A) lectin demonstrated aggregation at 1.56 μg/ml. LDC (rBC2-PD38) slightly affected haemagglutination at the very high concentrations of 25 μg/ml in mouse and 12.5 μg/ml in human samples. Each test contained n=3 technical replicates. Other blood types are shown in Supplementary Fig. S7. **C,** rBC2LC-N lectin staining of human red blood cells (Type A) contaminating clinical PDAC slides revealed that all red blood cells were negative, indicating that the rBC2LC-N lectin should not induce the aggregation of red blood cells. Notably, white blood cells (* with blue nucleus) were also negative for rBC2LC-N reactivity (scale bar, 100 μm). Other blood types are shown in Supplementary Fig. S8. **D,** The 50% lethal dose (LD_{50}) of rBC2LC-N alone and LDC by i.p (n=10 wild-type mice for each concentrations) and i.v. (n=7) administration were evaluated. The LD_{50} of a single i.p. and i.v.

administration of LDC was calculated to be 7.14 μg/mouse and 7.22 μg/mouse, respectively. By contrast, rBC2LC-N alone did not induce death at any dose tested up to 15 μg/mouse by both i.p. and i.v. administration.

Figure 4

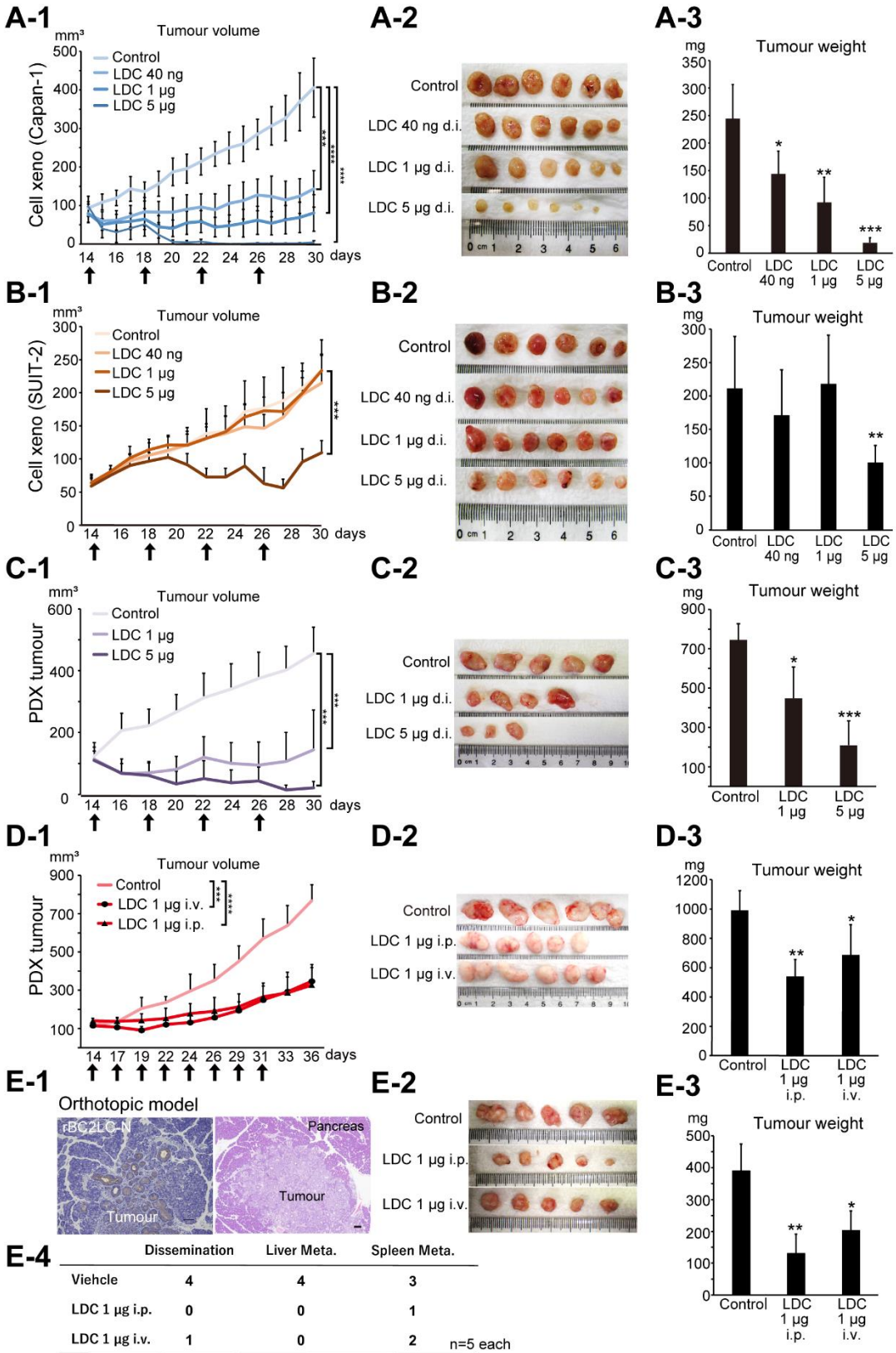

E-4

	Dissemination	Liver Meta.	Spleen Meta.
Viehcle	4	4	3
LDC 1 µg i.p.	0	0	1
LDC 1 µg i.v.	1	0	2

n=5 each

Fig. 4. *In vivo* effect of LDC (rBC2-PE38) on subcutaneous tumours in a mouse model after local injection. LDC was directly injected (i.v.) near the subcutaneous tumour 4 times, with one injection every 4 days (arrows in A-1, B-1). **A-1,** Subcutaneous tumour growth curves of Capan-1 xenografts. LDC significantly diminished the size of the xenograft tumours in a dose-dependent manner (n=6 biological replicates). **A-2, 3,** The objective weight of enucleated nodules obtained at day 30 also confirmed the prominent reduction of the tumour weight of Capan-1 xenografts by LDC. **B-1, 2, 3,** Subcutaneous SUIT-2 xenograft model (negative for the H type 1/3/4 glycan epitope). LDC d.i. did not induce a tumour reduction effect except at a dose of 5 μg/mouse. **C-1, 2, 3,** In the more clinically relevant PDX model with a moderately differentiated morphology, LDC d.i. also decreased the size of the subcutaneous nodules in a dose-dependent manner (n=5 biological replicates). **D-1, 2, 3,** A PDX model with a moderately differentiated morphology was tested for the effect of LDC via various injection root including i.p and i.v. The growth curves and average tumour weights after a total of 8 i.p. or i.v. administrations were significantly reduced. **E-1-4,** The effects of LDC (1 μg/mouse) administered via either the i.p. or the i.v. route for orthotopically transplanted Capan-1 tumours. H&E staining and rBC2CL-N lectin histochemistry demonstrated that Capan-1 cells (rBC2LC-N: positive) had invaded the mouse pancreas parenchyma

(negative) (scale bars, 100 μm). After 4 injections of LDC by either i.p. or the i.v., the tumour weights were significantly reduced (n=5 biological replicates.). The number of mice with metastases, including peritoneal dissemination, liver and spleen metastases, was decreased in the treatment groups (0-2/5 mice) relative to the control groups (3-4/5 mice). The results of statistical analysis by two-tailed unpaired Student's *t*-tests relative to control are indicated as follows: *P<0.05; **P<0.01; ***P<0.001; ****P<0.0001; n.s., not significant.

Figure 5

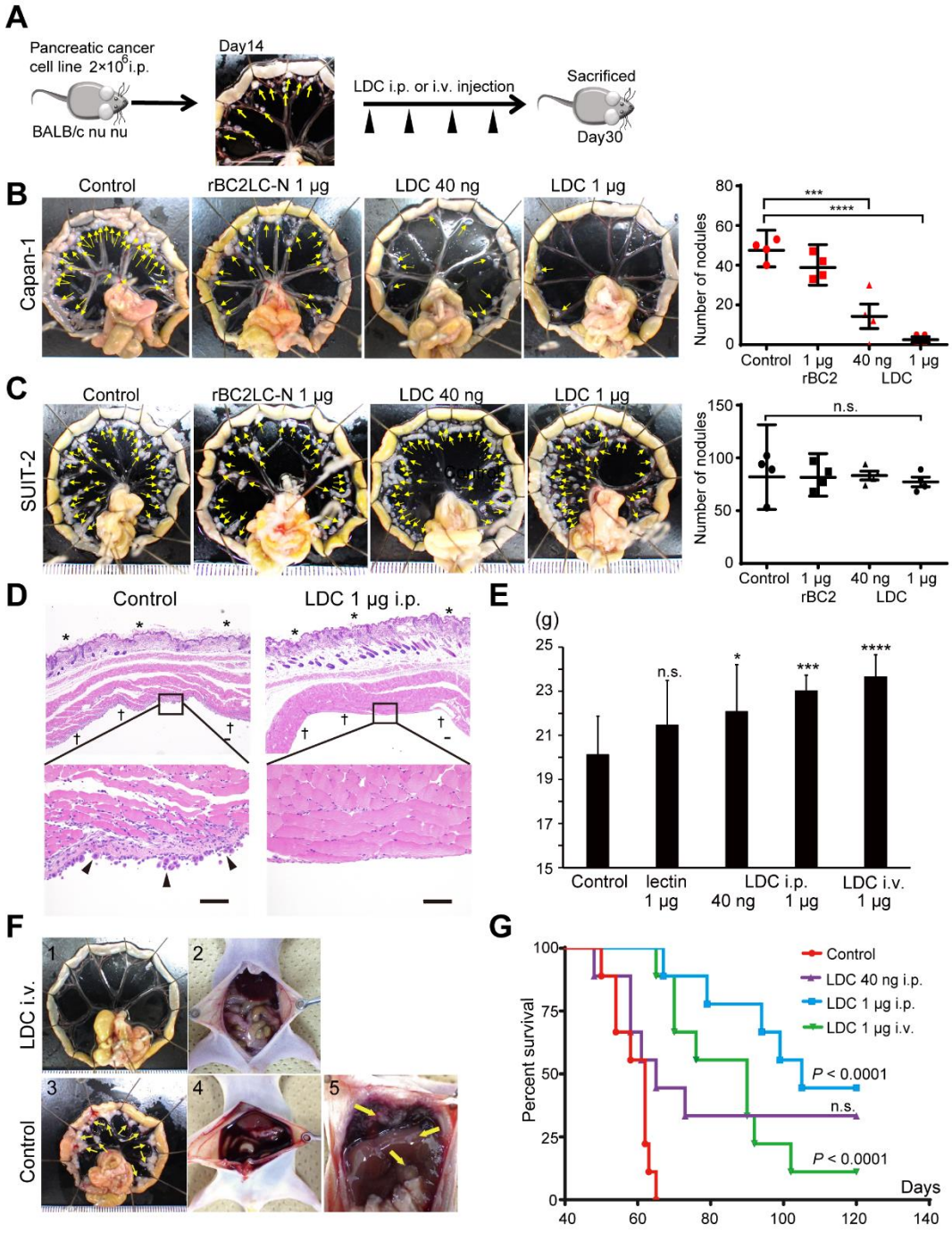

Fig. 5. Effectiveness of LDC for the treatment of PDAC peritoneal dissemination in a mouse model. A, At day 14 after i.p. injection of Capan-1 or SUIT-2 cells, many

opal-coloured nodules known as milky spots (arrows) were distributed on the peripheral margin of the small intestine (28). LDC was i.p. or i.v. injected 4 times. **B,** The mesenterium after treatment on day 30. In the Capan-1 model, numerous nodules (arrow) remained in the control and rBC2LC-N alone groups, whereas nodules were significantly and dose-dependently reduced in LDC-treated groups (n=4). **C,** The number of nodules was not altered in the SUIT-2 model. **D,** Microscopic observation of the resected abdominal wall (*, skin surface; †, peritoneum) revealed numerous disseminated cancer cells (arrows) in the control, whereas cancer cells were completely absent after i.p. injection of 1 μg of LDC (H&E staining, scale bar, 500 μm).

E, Body weight at day 45 was significantly reduced in the control and rBC2-lectin-without-toxin cohorts (n=9 biological replicates); n.s., not significant; *P<0.05; ***P<0.001; ****P<0.0001 (two-tailed unpaired Student's *t*-test). Intraperitoneal injection of LDC resulted in good weight gain, and body weight was comparable between the i.v. administration and i.p. administration of LDC cohorts. All mice were healthy and did not exhibit damage to non-cancerous epithelial cells of hollow or genitourinary organs, and the body weight of the mice was not affected by this treatment. **F-1**, Intravenous injection of LDC decreased peritoneal dissemination nodules of PDAC in the mouse model. **F-2,** Laparotomy in the 1 μg i.v. LDC cohort revealed no ascites and the mice

appeared slim and normal. **F-3,** The multiple peritoneal disseminated nodules (arrows) observed in the control. **F-4,** Laparotomy of controls revealed massive bloody ascites due to active disseminated cancer nodules. **F-5,** Disseminated nodules at the surface of the liver and nodules at the sub-diaphragmatic space (arrows). **G,** Kaplan-Meier survival curves after LDC treatment in the PDAC dissemination mouse model (n=9 for each group). The median number of days of survival in the control group (62 d) was significantly improved by i.p. injection of 1 μg of LDC, resulting in 90-d survival of 7/9 mice (median survival=105 d). Notably, i.v. injection of 1 μg of LDC conferred a comparable effect, with 90-d survival of 5/9 mice (median survival=90 d) (*P<0.05; ****P<0.0001; n.s., not significant by log-rank test).

Figure 6

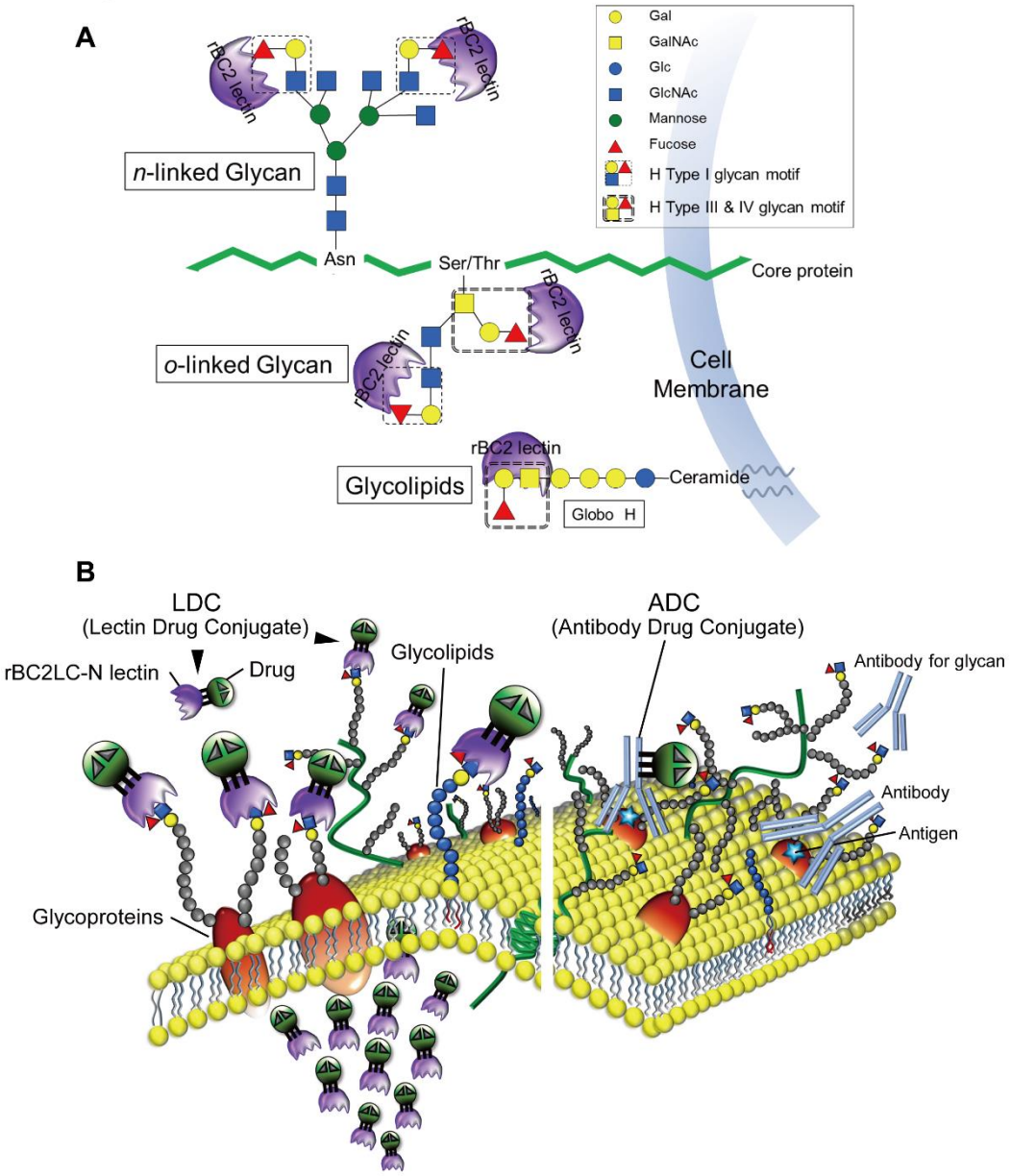

Fig. 6. A, Schema of rBC2LC-N lectin binding sites. rBC2LC-N is a TNF-like lectin molecule identified from the gram-negative bacterium *B. cenocepacia*, and this molecule is revealed to be a fucose-binding lectin (17). Precise survey using a glycan array containing 377 glycans revealed that the promising high-affinity ligands of rBC2LC-N are the H type 1 trisaccharide (Fucα1-2 Galβ1-3GlcNAc) and H type 3/4 trisaccharide

(Fucα1-2 Galβ1-3GalNAc), corresponding to two forms of the human blood group O determinant. The H type 1 trisaccharide motifs are present at the end of branched *N*-linked glycans and *O*-linked glycans. The proximate GalNAc in *O*-linked glycan could be a source of the H Type III trisaccharide motif. The end glycolipid, i.e., βGalNAc attached to the Globo H construct, could also be a source of the H type IV glycan motif. **B, Schema of rBC2LC-N lectin binding on the cancer cell surface. (right)** The previous failure of antibody-drug conjugates (ADC) strategies may be due to the one-to-one relationship between the cancer cell surface peptide antigen (blue star in brown glycoprotein) and the antibody, which results in the delivery of an insufficient amount of the drug to cancer cells. **(left)** In contrast, LDC binding sites could consist of multiple glycans on various glycoproteins and glycolipids, resulting in the delivery of more drug to the surface of target cells. In addition, the relatively large size of immunoglobulins tends to prevent effective internalization of antibody-based drugs; however, the relatively small (16-kDa) size of rBC2LC-N would facilitate effective endocytosis and the prominent cytocidal effect of LDC.

8. Supplementary materials

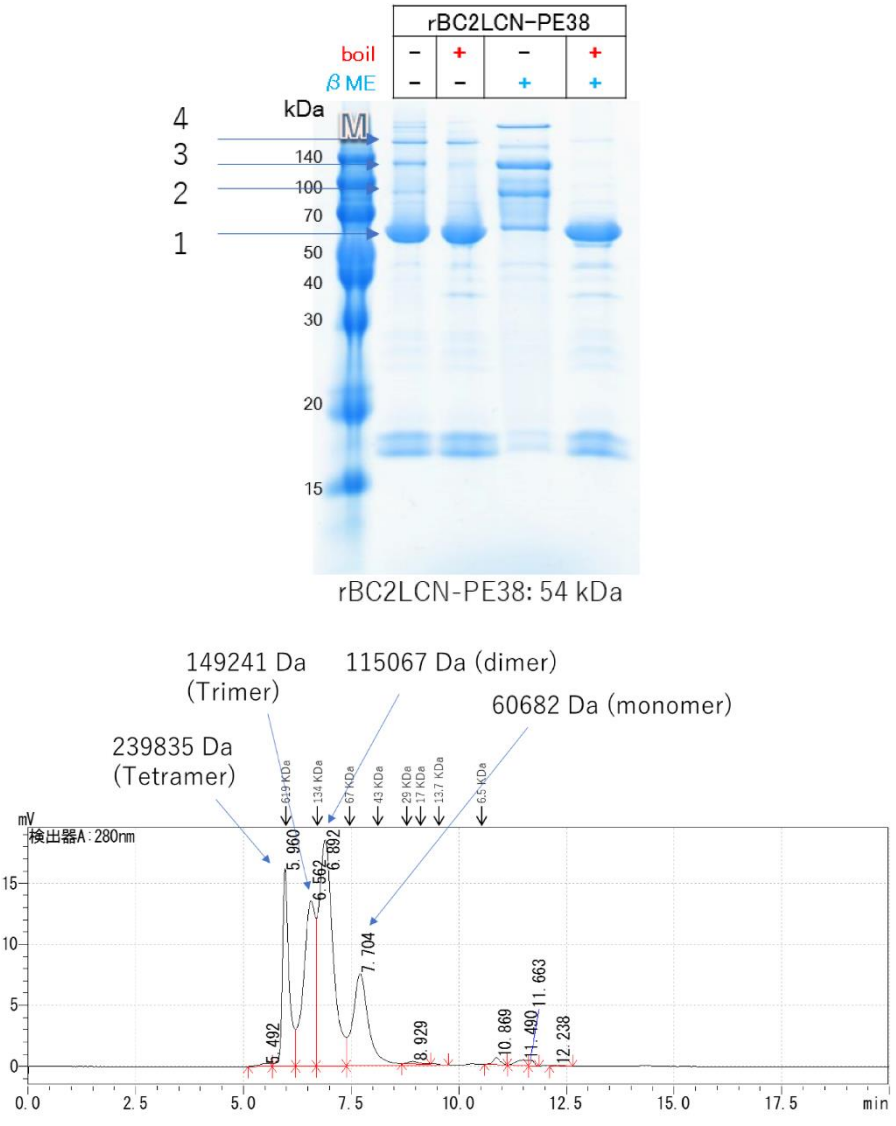

Supplementary Figure S1. SDS-PAGE and HPLC of rBC2LCN-PE38 (LDC).

The size exclusion-based FPLC demonstrated that rBC2LCN-PE38 forms various multimers, including monomers, dimers, trimers and tetramers. The values of peak voltage at 280 nm do not directly indicate the exact ratio of 4 monomers; however, dimers, trimers and tetramers appear to exist equally at substantial proportions. As SDS-PAGE

gels under various conditions demonstrate, the trimer is not the major form among the 4 multimers of rBC2LCN-PE38. However, the actual ratio among the 4 multimers in an *in vivo* setting remains controversial.

A

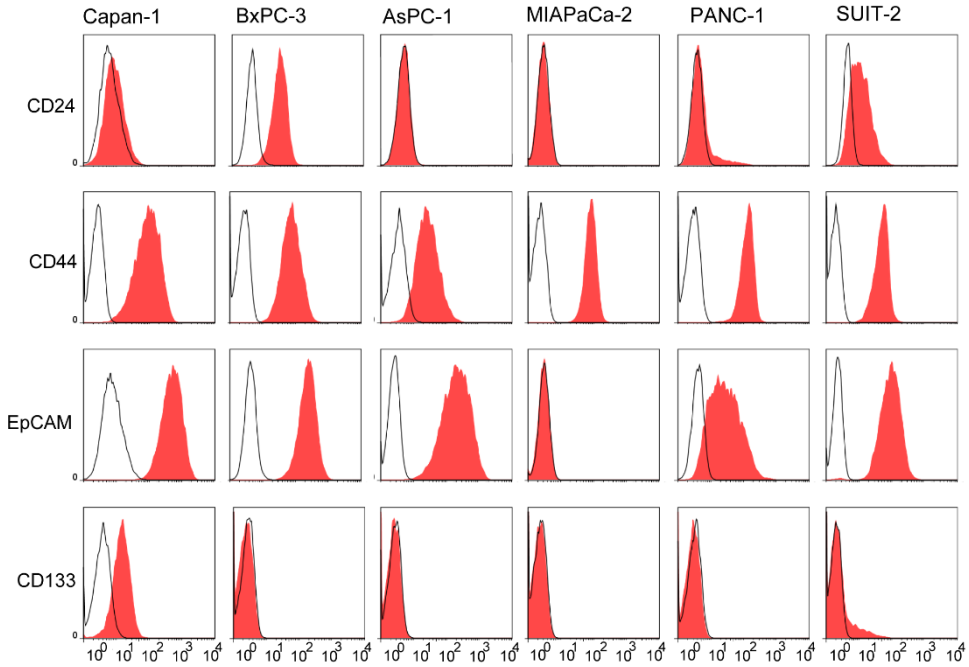

B

Antigen	Fluorescence	Clone	Brand	Isotype		Cat
CD24	FITC	ML5	BD Pharmingen	Mouse	IgG2aκ	555427
Isotype	FITC	G155-178	BD Pharmingen	Mouse	IgG2aκ	555573
CD44	APC	G44-26（C26）	BD Pharmingen	Mouse	IgG2bκ	559942
Isotype	APC	27-35	BD Pharmingen	Mouse	IgG2bκ	555745
EpCAM	PE	HEA-125	Miltenyi Biotech	Mouse	IgG1	130-091-253
Isotype	PE	IS5-21F5	Miltenyi Biotech	Mouse	IgG1	130-098-845
CD133/2	APC	293C3	Miltenyi Biotech	Mouse	IgG2b	130-090-854
Isotype	APC	IS6-11E5.11	Miltenyi Biotech	Mouse	IgG2b	130-098-890

C

	Morphology*		CSC markers			
	gland	**stroma**	**CD24**	**CD44**	**ESA**	**CD133**
Capan-1	++	++	−	+	+	+
BxPC-3	+	++	+	+	+	−
AsPC-1	+	−	−	+	+	−
MIAPACA-2	−	+	−	+	−	−
PANC-1	−	−	−	+	−	−
SUIT-2	−	−	−	+	+	−

*: the morphology of the mouse xenograft

Supplementary Figure S2. Analysis of cancer stem cell (CSC) marker expression in 6 PDAC cell lines. The expression of the known pancreatic CSC markers CD24, CD44, EpCAM, and CD133 (29,30) was analysed by flow cytometry. (**A**) Capan-1 cells

expressed 3 markers (CD44, EpCAM, and CD133), and BxPC-3 expressed 3 markers (CD24, CD44, and EpCAM). The remaining 4 cell lines were positive for only 1 or 2 markers. Note that CD133 was expressed only in Capan-1 cells. (**B**) The panel of the primary antibodies of CSC markers and isotypes used for negative control. (**C**) Summary of the morphology and CSC marker expression results for the 6 PDAC cell lines. We considered Capan-1 to be a valuable PDAC line that maintains morphology resembles clinical PDAC, i.e. the dominant presentation of well-to-moderately preserved gland formation and abundant stromal induction (31), together with CSC marker expressions. Thus, we have focused Capan-1 cell as the tester cell line that may represent PDAC glycan expressions.

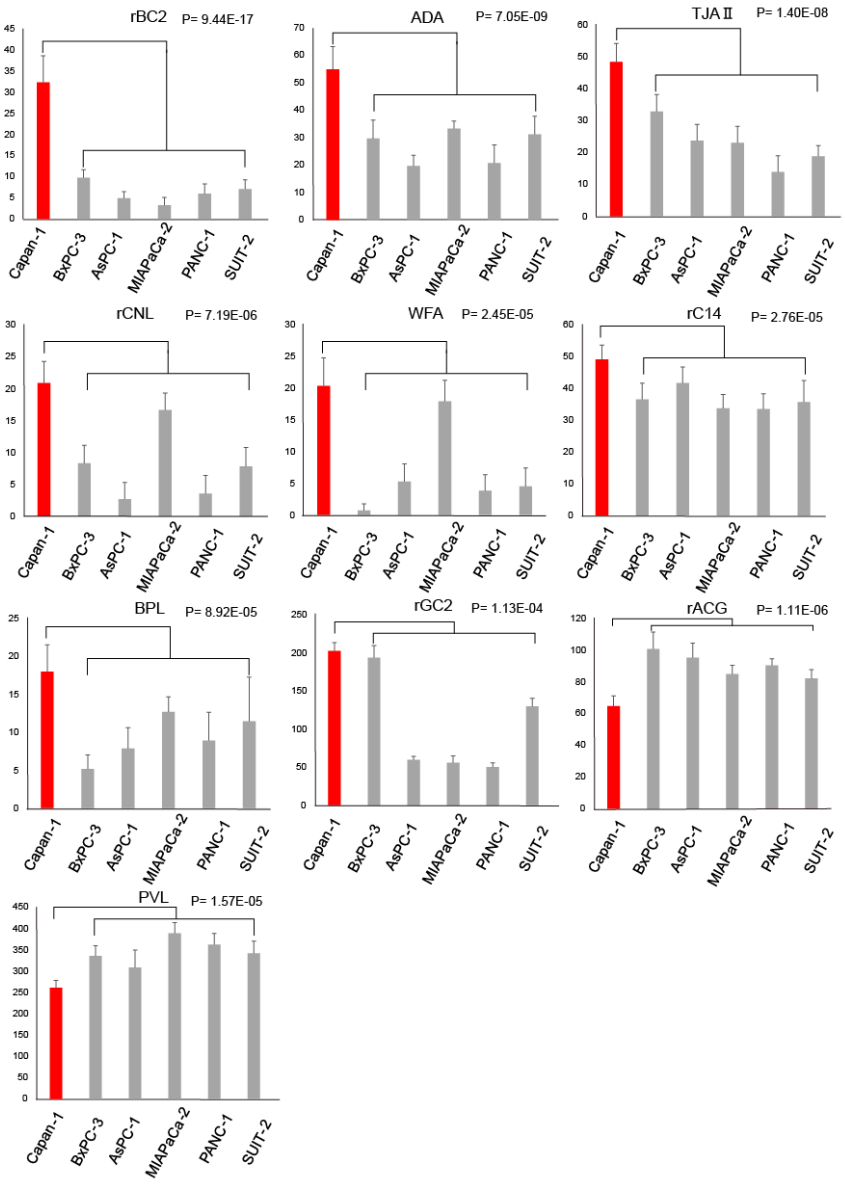

Supplementary Figure S3. Top 10 highlighted lectins that bind specifically to Capan-1 cells. The signal intensities yielded by the Capan-1 cell line on the lectin microarray were compared with those of 5 other cell lines. The top 10 lectins displaying specific differential reactivity in Capan-1 cells, including 8 lectins displaying increased reactivity and 2 lectins displaying decreased reactivity, are presented. The lectin exhibiting the most

prominent difference in reactivity was rBC2; it had a higher signal intensity in the Capan-1 cell line (32.21±6.89) than in the other cell lines (6.20±3.01, P=9.44E-17), followed by ADA (P=7.05E-09) and TJA II (P=1.40E-08). rACG and PVL exhibited significantly reduced signal intensity in Capan-1 cells.

Supplementary Table S1.

Ten highlighted lectins with specific reactivity to the pancreatic cell line 'Capan-1' as determined by high-density lectin microarray analysis.

			Mean signal intensity		
	Lectins	Complement sugar chain	Capan-1	Other lines	P value
1	rBC2LC-N	Fuc α1-2 (H) Galβ1-3GlcNac (H type 1/3/4)	32.3 ± 6.9	6.2 ± 3.0	9.44E-17
2	ADA	α2-6 Sia, Forssman, A, B	54.9 ± 9.0	26.9 ± 8.1	7.05E-09
3	TJAII	α1-2 Fuc, LacDiNAc	48.3 ± 6.3	22.5 ± 8.1	1.40E-08
4	rACG	α2-3 Sia	64.7 ± 7.2	90.7 ± 10.2	1.11E-06
5	rCNL	α,β GalNAc (A, Tn, LacDiNAc)	20.9 ± 3.7	7.9 ± 5.8	7.19E-06
6	PVL	Sia, GlcNAc	261.1 ± 19.1	347.4 ± 40.8	1.57E-05
7	WFA	Terminal GalNac, LacDiNAc	20.4 ± 4.8	6.5 ± 6.6	2.45E-05
8	rC14	Branched LacNAc	49.2 ± 4.9	36.3 ± 6.1	2.76E-05
9	BPL	Galβ1-3GlcNAc (GalNAc), α/β GalNAcNAc	18.0 ± 3.8	9.3 ± 4.5	8.92E-05
10	rGC2	α1-2Fuc (H), α GalNAc (A), αGal (B)	203.3 ± 12.0	98.4 ± 58.0	1.13E-04

Fuc: fucose, Gal: galacctose, GalNAc: N-acetylgalactosamine, GlcNAc: N-acetylglucosamine, Sia: silalic acid, LacNAc: N-acetyl-lactosamine

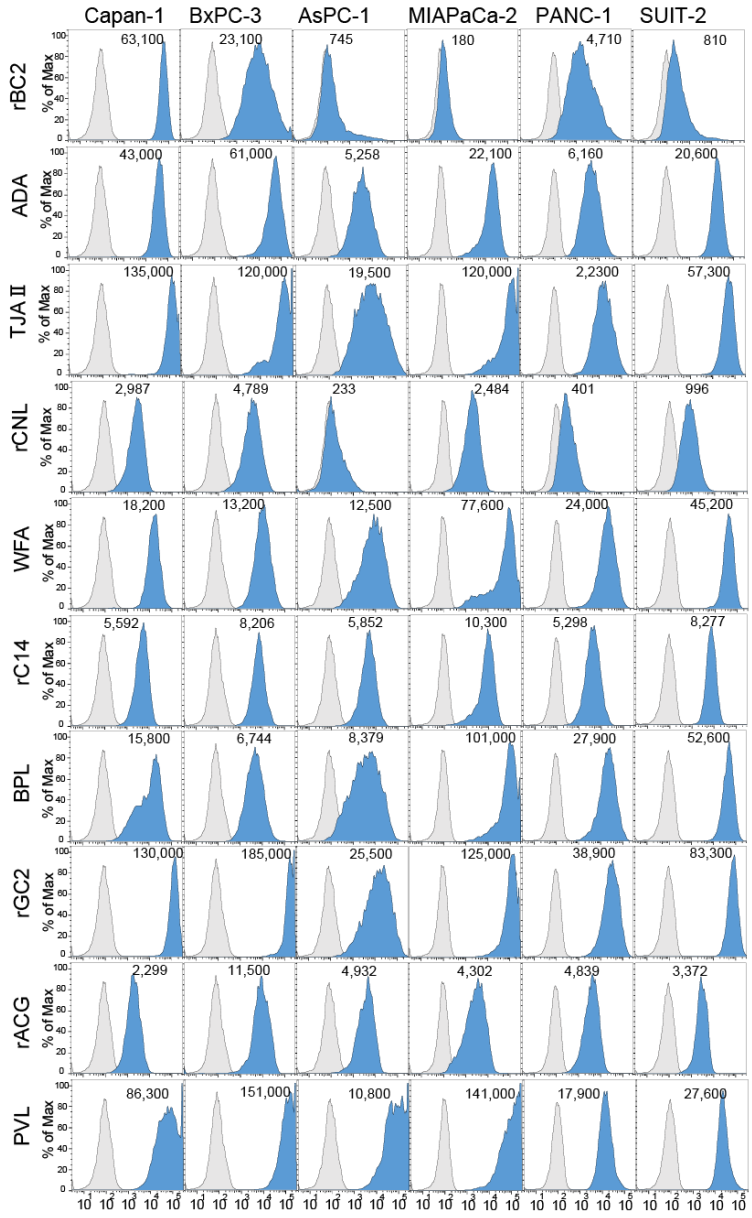

Supplementary Figure S4. Evaluation of the affinity between lectins and PDAC cell lines by flow cytometry using fluorescent labelling of the 10 lectins that were highlighted by lectin microarray. The results obtained with Capan-1 cells were consistent with the results of the lectin microarray analysis. In contrast, the flow cytometry analysis results for the other 9 lectins were not comparable to the lectin

microarray data, likely because flow cytometry reflects only cell-surface reactivity whereas lectin microarrays reflect the reactivity of whole-cell lysates.

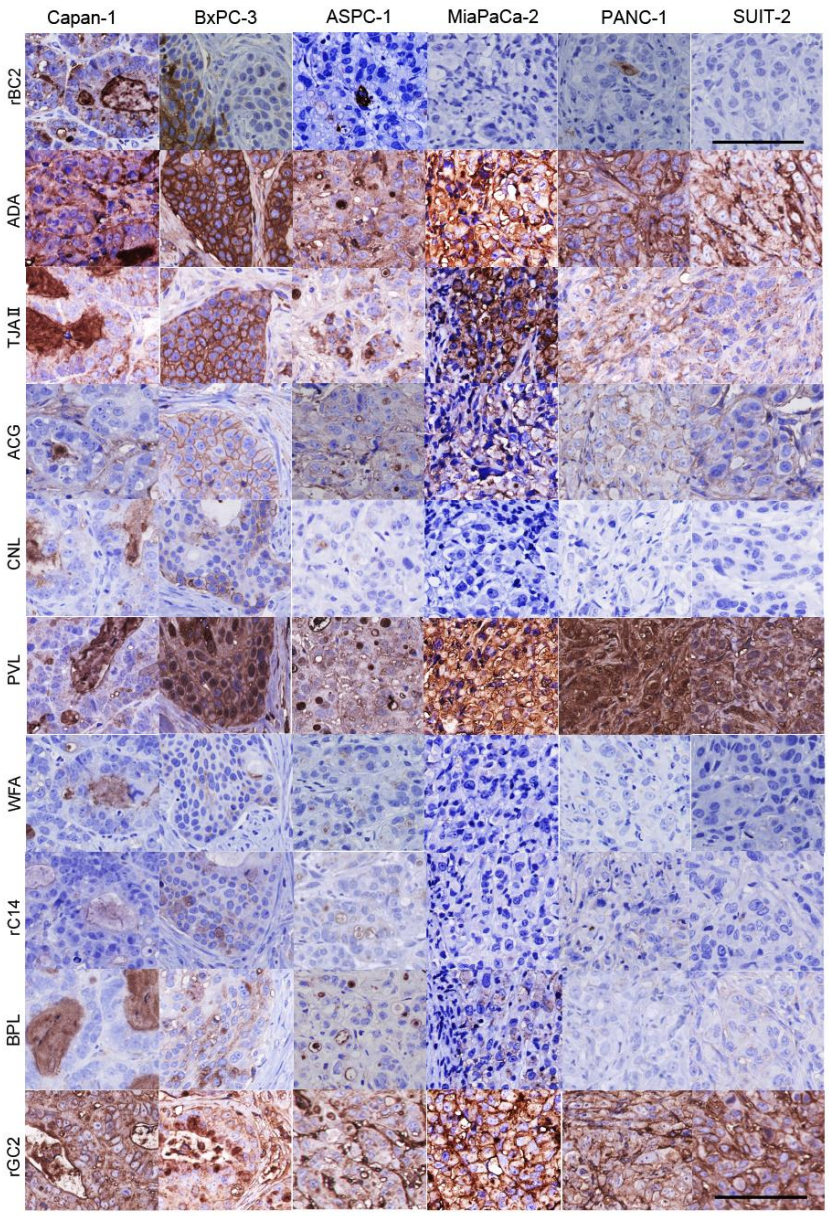

Supplementary Figure S5. Lectin histochemistry of mouse PDAC xenograft models.

To confirm the results of the lectin microarray analysis, lectin histochemistry using 10 HRP-labelled lectins was performed on xenograft nodules derived from the 6 PDAC cell lines. rBC2 exhibited strong membranous staining in Capan-1 xenografts and mosaic staining in BxPC-3 xenografts, whereas the remaining 4 cell lines were negative for rBC2.

The observations for rBC2 lectin were in good agreement with the results of the lectin microarray and live-cell staining analyses. In contrast, staining of the other 9 lectins did not support specific lectin affinity of the Capan-1 cell line (scale bars, 100 μm).

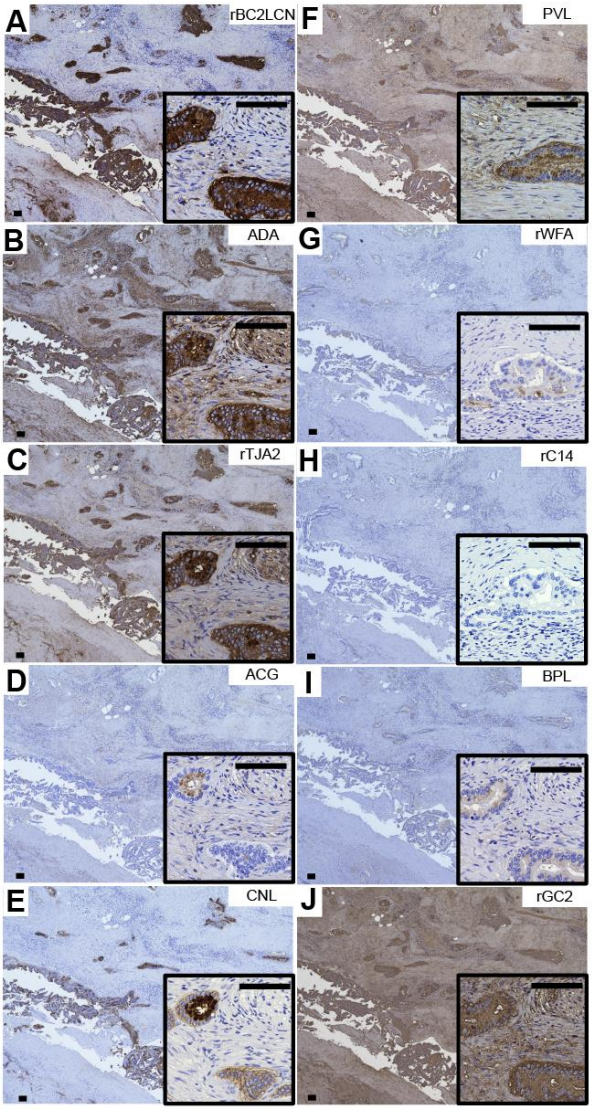

Supplementary Figure S6. Histochemical analysis of the top 10 highlighted lectins in a single PDAC sample. Histochemistry for 10 lectins was performed on serial sections of a clinical PDAC sample. All lectins were labelled by horseradish peroxidase (HRP). All lectins except rC14 displayed affinity for PDAC cells. The rACG, rWFA and rBPL lectins (D, G and I) had weak affinity for cancer cells. The rADA, rTJA2, rPVL and rGC2 lectins (B, C, F and J) had affinity for both cancer cells and stromal cells. The rBC2LC-

N and rCNL lectins (A, E) clearly recognized cancer cells and had no affinity for stromal cells. However, rCNL likely has a higher affinity for mucus discharges from cancer cells (E). Among the 10 lectins, rBC2LC-N lectin was identified as an excellent lectin for recognizing PDAC cells (scale bars, 100 μm).

Supplementary Table S2. Summary of recently reported immunotoxins and LDC with their targets and IC50s (32-48).

Target antigen	malignancy	Agents name	Toxin	IC50	Reference
IL-2R	**CLL**	Anti-Tac(Fv)-PE40KDEL	PE	**1.2~9 ng/ml**	Kreitman, R. J., et al. 1992
GP185/HER2	**Breast Ovary**	Saporin Anti-GP185/HER2 IT	SAP	**0.43~1.1 nM**	Tecce, R., et al. 1993
IL-2R	**ATL CLL**	Anti-Tac(FV)-PE40	PE	**0.04~ >1000 ng/ml**	Kreitman, R. J., et al. 1994
NCAM	**Lung cancer**	SEN7-PE	PE	**22~85 pM**	Zangemeister, U., et al. 1994
CD80	**Hodgikin's**	Anti-B7-1-saporina	SAP	**3.2 ng/ml**	Vooijs, W. C., et al. 1997
GRP	**Lung**	DAB389GRP	DT	**9.5 pM**	vanderSpek, J. C., et al. 1997
E4	**Prostate**	E4PE35-KDEL	PE	**0.3-20 ng/ml**	Essand, M. and I. Pastan 1998
CD30	**Hodgikin's**	Ki-4(scFv)-ETA	PE	**43 pM**	Klimka, A., et al. 1999
CD22	**lymphoma**	RFB4(dsFv)-PE38	PE38	**0.4 ng/ml**	Kreitman, R. J., et al 1999
IL-13R	**Head and Neck**	IL13-PE38	PE38	**3~7 ng/ml**	Kawakami, K., et al. 2001
IL-4R	**Pancreas**	IL4-PE38	PE38	**0.3~0.5 ng/ml**	Kawakami, K., et al. 2002
EpCAM	**Head and Neck**	4D5MOCB-ETA	PE	**0.005~0.2 pM**	Di Paolo, C., et al. 2003
GCSF	**AML**	DTU2GSF	DT	**5.8~34.7 pM**	Abi-Habib, R. J., et al. 2004
CD19	**Blood**	FMC63(Fv)-PE38	PE38	**0.6-14 ng/ml**	Du, X., et al. 2008
CD22	**Blood**	RFB4(Fv)-PE38	PE38	**50-550 ng/ml**	Du, X., et al. 2008
CD22	**Blood**	B3(dsFv)-PE38	PE38	**0.1-2.5 ng/ml**	Weldon, J. E., et al. 2009
CD30	**Lymphoma**	SGN-35	MMAE	**1.3 ng/ml**	Okeley, N. M., et al. 2010
mesothelin	**Pancreas**	RG7787	PE24	**1.38~33.28 ng/ml**	Hollevoet, K., et al. 2014
HER2	**Breast**	4D5scFv-ETA	PE40	**22 nM**	Sokolova, E. A., et al. 2014
CD71	**Pancreas**	HB21(Fv)-PE40	PE40	**3~3.7 ng/ml**	Hollevoet, K., et al. 2015
Glypican-3	**liver**	HN3-PE38	PE38	**0.068 nM~**	Gao, W., et al. 2015
H type 1/3/4	**Pancreas**	rBC2LCN-PE38	PE38	**1.04 pg/ml (0.0195 pM)**	Author

CLL; chronic lymphocytic leukemia, ATL: adult T-cell leckemia, PE; pseudomonas aerginosa exotoxin, DT; diphteria toxin, SAP; plant toxin saporin 6, MMAE; monomethylauristatin E,

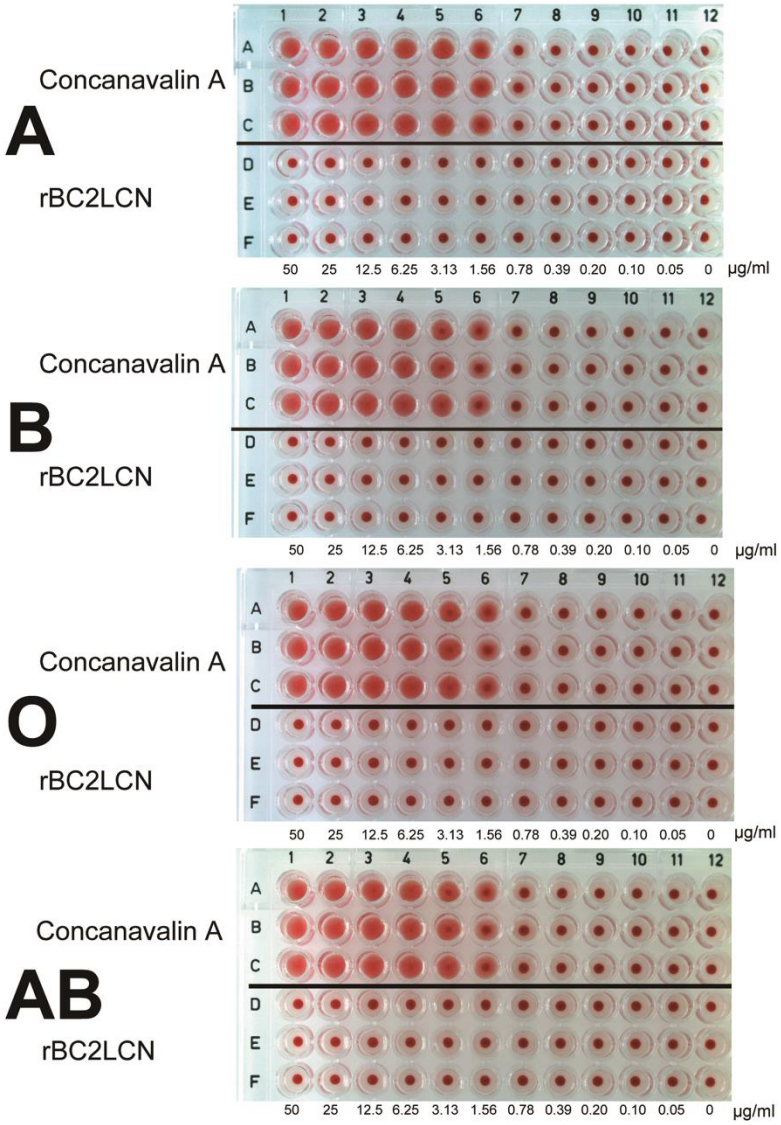

Supplementary Figure S7.

Representative images of assays of erythrocytes from human volunteers. There was no agglutination with the rBC2 lectin for any blood type (A, B, AB and O), in contrast to the obvious agglutination at 0.78 µg/ml Concanavalin A, a positive-control lectin. This result demonstrates that not all lectins possess hemagglutination activity, which would prevent the use of lectins as *in vivo* therapeutic carriers, and that a subgroup of lectins, including

rBC2, can be utilized as therapeutic carriers. Each test involved n=3 technical replicates.

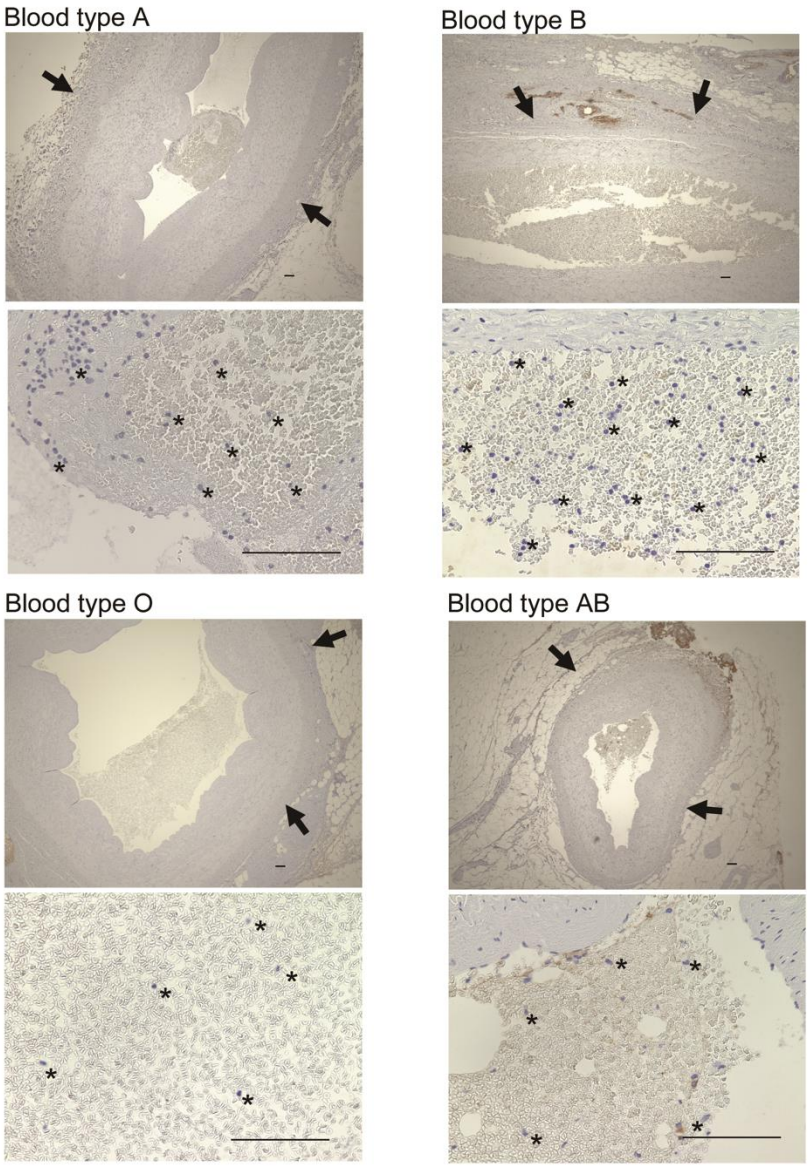

Supplementary Figure S8.

Clinical PDAC slides stained with H&E were examined for contaminating large arterial vessels (arrows), and serial unstained slides were subjected to HRP-labelled rBC2LC-N lectin histochemistry. All red blood cells in the vessels and white blood cells of patients of all 4 blood types (A, B, AB and O) were negative, indicating that red blood cells are negative for the H type 1/3/4 motif. This result further indicates that the intravenous

administration of rBC2LC-N has little risk of causing hemagglutination (scale bars, 100 μm).

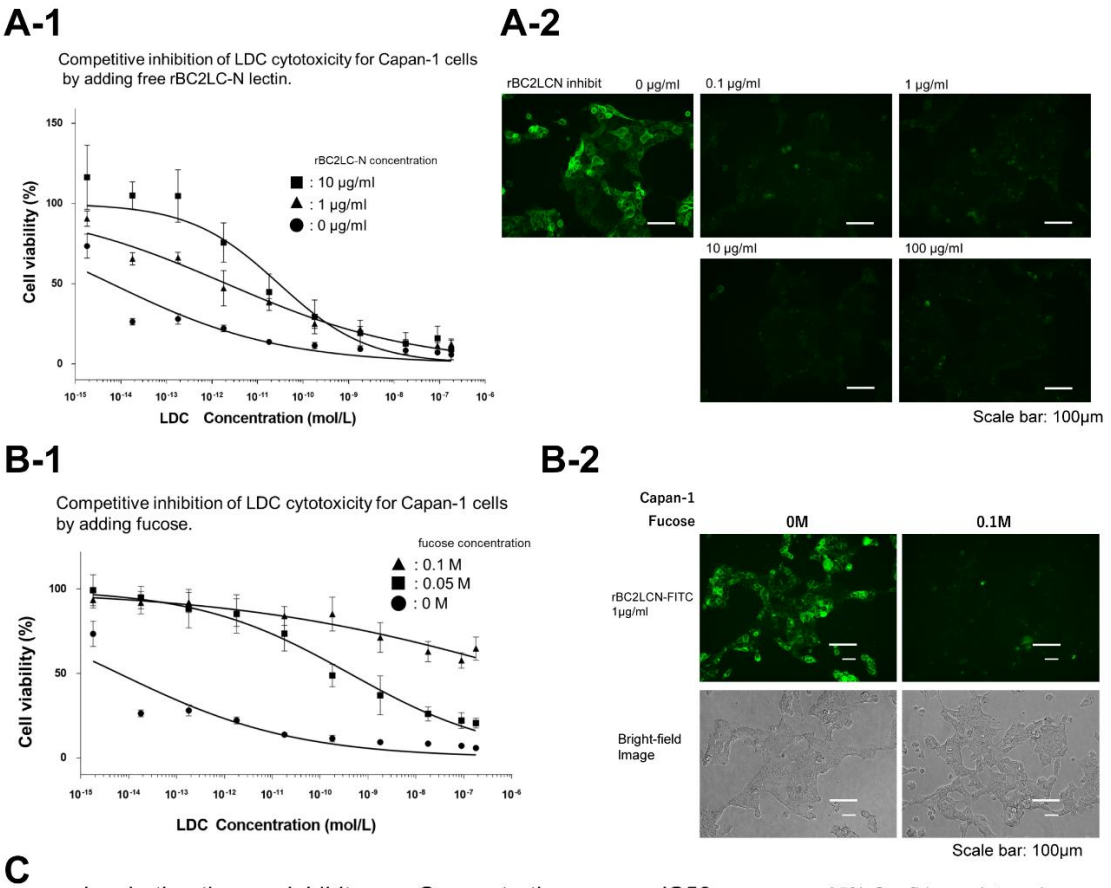

C

Incubation time	Inhibitor	Concentration	IC50	95% Confidence Intervals
24h	none	—	3.33E-09	1.039e-009 to 1.067e-008
48h	none	—	1.37E-13	2.665e-014 to 7.070e-013
72h	none	—	7.11E-15	1.776e-015 to 2.132e-014
48h+24h	none	—	2.31E-14	3.553e-015 to 1.350e-013
72h	rBC2LC-N	1 μg/ml	2.07E-12	9.308e-013 to 4.613e-012
72h	rBC2LC-N	10 μg/ml	2.92E-11	7.875e-012 to 1.085e-010
72h	fucose	0.05 M	4.11E-10	1.414e-010 to 1.197e-009
72h	fucose	0.1 M	2.77E-06	1.085e-007 to 7.093e-005

Supplementary Figure S9. The validation of the specificity of rBC2LC-N lectin by competition assay. MTT assay of LDC were carried out by adding competitive agents. A-1; free rBC2LC-N and B-1; target glycan (=fucose), demonstrating both were inhibited in dose dependent manner. Live cells (Capan-1) was incubated with fluorescent labelled rBCLC-N after 30 min incubation with free rBC2LC-N (A-2) and target glycan (=fucose.

B-2). Green signal were competitively inhibited by these agents. The IC50 value were re-checked in different evaluation times and those by competitive inhibition assay were summarized in C.

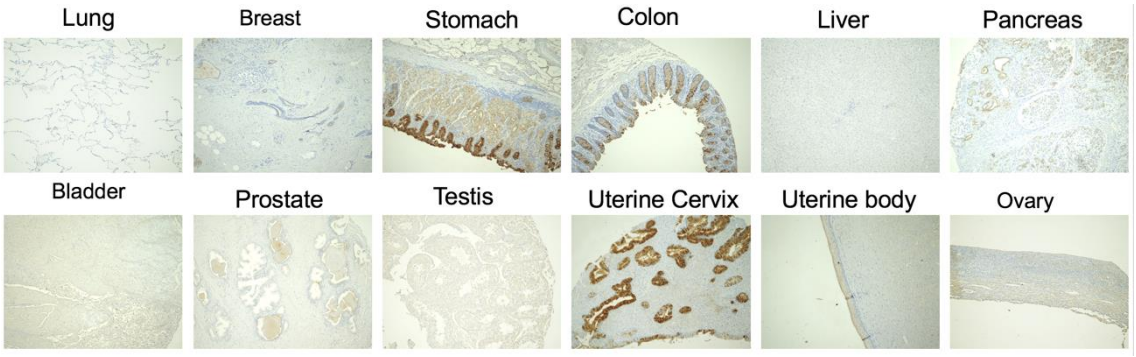

Supplementary Figure S10. The rBC2LC-N lectin reactivity to human organs. Formalin-Fixed human tissues were stained with rBC2LC-N lectin. Positive reactivity to rBC2LC-N in epithelial cells on the internal surface of the hollow organs (strongly in the stomach, colon and uterine cervix) were evident, hence the staining in other organs were scant.

9. References

1. Teicher BA, Doroshow JH. The promise of antibody-drug conjugates. *N Engl J Med* **2012**;367:1847-8.

2. Sharkey RM, McBride WJ, Cardillo TM, Govindan SV, Wang Y, Rossi EA, *et al.* Enhanced Delivery of SN-38 to Human Tumor Xenografts with an Anti-Trop-2-SN-38 Antibody Conjugate (Sacituzumab Govitecan). *Clin Cancer Res* **2015**;21:5131-8.

3. Zhu Y, Choi SH, Shah K. Multifunctional receptor-targeting antibodies for cancer therapy. *Lancet Oncol* **2015**;16:e543-54.

4. Tarbell JM, Cancel LM. The glycocalyx and its significance in human medicine. *J Intern Med* **2016**;280:97-113.

5. Pinho SS, Reis CA. Glycosylation in cancer: mechanisms and clinical implications. *Nat Rev Cancer* **2015**;15:540-55.

6. Christiansen MN, Chik J, Lee L, Anugraham M, Abrahams JL, Packer NH. Cell surface protein glycosylation in cancer. *Proteomics* **2014**;14:525-46.

7. Reticker-Flynn NE, Bhatia SN. Aberrant glycosylation promotes lung cancer metastasis through adhesion to galectins in the metastatic niche. *Cancer Discov* **2015**;5:168-81.

8. Dingjan T, Spendlove I, Durrant LG, Scott AM, Yuriev E, Ramsland PA. Structural biology of antibody recognition of carbohydrate epitopes and potential uses for targeted cancer immunotherapies. *Mol Immunol* **2015**;67:75-88.

9. Rahib L, Smith BD, Aizenberg R, Rosenzweig AB, Fleshman JM, Matrisian LM. Projecting cancer incidence and deaths to 2030: the unexpected burden of thyroid, liver, and pancreas cancers in the United States. *Cancer Res* **2014**;74:2913-21.

10. Sharon N, Lis H. History of lectins: from hemagglutinins to biological recognition molecules. *Glycobiology* **2004**;14:53r-62r.

11. Belardi B, Bertozzi CR. Chemical Lectinology: Tools for Probing the Ligands and Dynamics of Mammalian Lectins In Vivo. *Chem Biol* **2015**;22:983-93.

12. Rabinovich GA, Croci DO. Regulatory circuits mediated by lectin-glycan interactions in autoimmunity and cancer. *Immunity* **2012**;36:322-35.

13. Deer EL, Gonzalez-Hernandez J, Coursen JD, Shea JE, Ngatia J, Scaife CL, *et al.* Phenotype and genotype of pancreatic cancer cell lines. *Pancreas* **2010**;39:425-35.

14. Kuno A, Uchiyama N, Koseki-Kuno S, Ebe Y, Takashima S, Yamada M, *et al.* Evanescent-field fluorescence-assisted lectin microarray: a new strategy for glycan profiling. *Nat Methods* **2005**;2:851-6.

15. Hermann PC, Huber SL, Herrler T, Aicher A, Ellwart JW, Guba M, *et al.* Distinct populations of cancer stem cells determine tumor growth and metastatic activity in human pancreatic cancer. *Cell Stem Cell* **2007**;1:313-23.

16. Li C, Heidt DG, Dalerba P, Burant CF, Zhang L, Adsay V, *et al.* Identification of pancreatic cancer stem cells. *Cancer Res* **2007**;67:1030-7.

17. Sulak O, Cioci G, Delia M, Lahmann M, Varrot A, Imberty A, *et al.* A TNF-like trimeric lectin domain from Burkholderia cenocepacia with specificity for fucosylated human histo-blood group antigens. *Structure* **2010**;18:59-72.

18. Tateno H, Onuma Y, Ito Y, Minoshima F, Saito S, Shimizu M, *et al.* Elimination of tumorigenic human pluripotent stem cells by a recombinant lectin-toxin fusion protein. *Stem Cell Reports* **2015**;4:811-20.

19. Alewine C, Hassan R, Pastan I. Advances in anticancer immunotoxin therapy. *Oncologist* **2015**;20:176-85.

20. Tateno H, Toyota M, Saito S, Onuma Y, Ito Y, Hiemori K, *et al.* Glycome diagnosis of human induced pluripotent stem cells using lectin microarray. *J Biol Chem* **2011**;286:20345-53.

21. Zhang W, Zhu ZY. Structural modification of H histo-blood group antigen. *Blood Transfus* **2015**;13:143-9.

22. Stanley P, Cummings RD. Structures Common to Different Glycans. In: Ajit Varki, Cummings RD, Esko JD, et al., editors. Essentials of Glycobiology 2nd edition. New York: Cold Spring Harbor Laboratory Press; 2009.

23. Matsumura Y, Maeda H. A new concept for macromolecular therapeutics in cancer chemotherapy: mechanism of tumoritropic accumulation of proteins and the antitumor agent smancs. *Cancer Res* **1986**;46:6387-92.

24. Akashi Y, Oda T, Ohara Y, Miyamoto R, Hashimoto S, Enomoto T, *et al.* Histological advantages of the tumor graft: a murine model involving transplantation of human pancreatic cancer tissue fragments. *Pancreas* **2013**;42:1275-82.

25. Akashi Y, Oda T, Ohara Y, Miyamoto R, Kurokawa T, Hashimoto S, *et al.* Anticancer effects of gemcitabine are enhanced by co-administered iRGD

peptide in murine pancreatic cancer models that overexpressed neuropilin-1. *Br J Cancer* **2014**;110:1481-7.

26. Bach PB. New Math on Drug Cost-Effectiveness. *N Engl J Med* **2015**;373:1797-9.

27. Hu D, Tateno H, Hirabayashi J. Lectin engineering, a molecular evolutionary approach to expanding the lectin utilities. *Molecules* **2015**;20:7637-56.

28. Hagiwara A, Takahashi T, Sawai K, Taniguchi H, Shimotsuma M, Okano S*, et al.* Milky spots as the implantation site for malignant cells in peritoneal dissemination in mice. *Cancer Res* **1993**;53:687-92.

29. Li C, Heidt DG, Dalerba P, Burant CF, Zhang L, Adsay V*, et al.* Identification of pancreatic cancer stem cells. Cancer Res 2007;67:1030-7.

30. Hermann PC, Huber SL, Herrler T, Aicher A, Ellwart JW, Guba M*, et al.* Distinct populations of cancer stem cells determine tumor growth and metastatic activity in human pancreatic cancer. Cell Stem Cell 2007;1:313-23.

31. Deer EL, Gonzalez-Hernandez J, Coursen JD, Shea JE, Ngatia J, Scaife CL*, et al.* Phenotype and genotype of pancreatic cancer cell lines. *Pancreas* **2010**;39:425-35.

32. Hollevoet K, Mason-Osann E, Muller F, Pastan I. Methylation-associated partial down-regulation of mesothelin causes resistance to anti-mesothelin immunotoxins in a pancreatic cancer cell line. PLoS One **2015**;10:e0122462.

33. Gao W, Tang Z, Zhang YF, Feng M, Qian M, Dimitrov DS, *et al.* Immunotoxin targeting glypican-3 regresses liver cancer via dual inhibition of Wnt signalling and protein synthesis. Nature communications **2015**;6:6536.

34. Hollevoet K, Mason-Osann E, Liu XF, Imhof-Jung S, Niederfellner G, Pastan I. In vitro and in vivo activity of the low-immunogenic antimesothelin immunotoxin RG7787 in pancreatic cancer. Mol Cancer Ther **2014**;13:2040-9.

35. Okeley NM, Miyamoto JB, Zhang X, Sanderson RJ, Benjamin DR, Sievers EL, *et al.* Intracellular activation of SGN-35, a potent anti-CD30 antibody-drug conjugate. Clin Cancer Res **2010**;16:888-97.

36. Weldon JE, Xiang L, Chertov O, Margulies I, Kreitman RJ, FitzGerald DJ, *et al.* A protease-resistant immunotoxin against CD22 with greatly increased activity against CLL and diminished animal toxicity. Blood **2009**;113:3792-800.

37. Du X, Beers R, Fitzgerald DJ, Pastan I. Differential cellular internalization of anti-CD19 and -CD22 immunotoxins results in different cytotoxic activity. Cancer Res **2008**;68:6300-5.

38. Abi-Habib RJ, Liu S, Bugge TH, Leppla SH, Frankel AE. A urokinase-activated recombinant diphtheria toxin targeting the granulocyte-macrophage colony-stimulating factor receptor is selectively cytotoxic to human acute myeloid leukemia blasts. Blood **2004**;104:2143-8.

39. Di Paolo C, Willuda J, Kubetzko S, Lauffer I, Tschudi D, Waibel R, *et al.* A recombinant immunotoxin derived from a humanized epithelial cell adhesion molecule-specific single-chain antibody fragment has potent and selective antitumor activity. Clin Cancer Res **2003**;9:2837-48.

40. Kawakami K, Kawakami M, Husain SR, Puri RK. Targeting interleukin-4 receptors for effective pancreatic cancer therapy. Cancer Res **2002**;62:3575-80.

41. Kawakami K, Kawakami M, Joshi BH, Puri RK. Interleukin-13 receptor-targeted cancer therapy in an immunodeficient animal model of human head and neck cancer. Cancer Res **2001**;61:6194-200.

42. Klimka A, Barth S, Matthey B, Roovers RC, Lemke H, Hansen H, *et al.* An anti-CD30 single-chain Fv selected by phage display and fused to Pseudomonas exotoxin A (Ki-4(scFv)-ETA') is a potent immunotoxin against a Hodgkin-derived cell line. Br J Cancer **1999**;80:1214-22.

43. Essand M, Pastan I. Anti-prostate immunotoxins: cytotoxicity of E4 antibody-Pseudomonas exotoxin constructs. Int J Cancer **1998**;77:123-7.

44. Vooijs WC, Otten HG, van Vliet M, van Dijk AJ, de Weger RA, de Boer M, *et al.* B7-1 (CD80) as target for immunotoxin therapy for Hodgkin's disease. Br J Cancer **1997**;76:1163-9.

45. Zangemeister-Wittke U, Collinson AR, Frosch B, Waibel R, Schenker T, Stahel RA. Immunotoxins recognising a new epitope on the neural cell adhesion molecule have potent cytotoxic effects against small cell lung cancer. Br J Cancer **1994**;69:32-9.

46. Kreitman RJ, Bailon P, Chaudhary VK, FitzGerald DJ, Pastan I. Recombinant immunotoxins containing anti-Tac(Fv) and derivatives of Pseudomonas exotoxin produce complete regression in mice of an interleukin-2 receptor-expressing human carcinoma. Blood **1994**;83:426-34.

47. Tecce R, Digiesi G, Savarese A, Trizio D, Natali PG. Characterization of cytotoxic activity of saporin anti-gp185/HER-2 immunotoxins. Int J Cancer **1993**;55:122-7.

48. Kreitman RJ, Chaudhary VK, Kozak RW, FitzGerald DJ, Waldman TA, Pastan I. Recombinant toxins containing the variable domains of the anti-Tac monoclonal

antibody to the interleukin-2 receptor kill malignant cells from patients with chronic lymphocytic leukemia. Blood **1992**;80:2344-52.

10. Acknowledgements

本研究は、著者が筑波大学人間総合科学研究科疾患制御医学専攻博士課程在学中に、同大学人間総合科学研究科大河内信弘教授ならびに小田竜也教授、および、共同研究機関である国立研究開発法人産業技術総合研究所創薬基盤部門細胞グライコーム標的技術グループの舘野浩章先生、平林　淳先生の元で行ったものです。このような機会を与えて下さった両教授、産総研の両先生方に感謝申し上げます。また、日頃の研究において助言、助力頂いた同研究室の小澤祐介先生、木村聡大先生、実験助手の高橋亜子さん、同研究室の卒業生で実験指導、助言を賜りました黒川友博先生、稲垣勇紀先生に感謝申し上げます。また実験に助言を賜りましたエーザイ株式会社オンコロジーユニット立野　翔先生、松井順二先生、筑波大学病院病理診断部野口雅之先生、坂下信悟先生、論文執筆にあたり助言を賜りました筑波大学生命科学動物資源センター西村　暹先生、オックスフォード大Eric O’Neill先生、コロンビア大菅原一樹先生に感謝申し上げます。